TAMPEREEN TEKNILLINEN YLIOPISTO
TAMPERE UNIVERSITY OF TECHNOLOGY

LAURI NIITTYMÄKI

FLEXIBLE CFD SIMULATION MODEL OF A THIN VAPOR CHAMBER FOR MOBILE APPLICATIONS

Master of Science thesis

Examiner: prof. Veli-Tapani Kuokkala
Examiner and topic approved by the
Faculty Council of the Faculty of
Engineering Sciences
on 3rd February 2016

ABSTRACT

LAURI NIITTYMÄKI: Flexible CFD simulation model of a thin vapor chamber for mobile applications
Tampere University of technology
Master of Science Thesis, 47 pages
October 2016
Master's Degree Programme in Materials Science
Major: Materials Research
Examiner: Professor Veli-Tapani Kuokkala

Keywords: vapor chamber, behavioral model, thermal management, heat spreader, simulation, mobile, CFD

Heat loads produced by electronics inside a mobile device are increasing as more computing power is packed into them. During the design phase of a product, these loads have to be taken into account. Simulations provides a way to try different designs more quickly, and built-in optimization tools help to find the most suitable solution.

Vapor chambers are thin heat spreaders that offer very high spreading capabilities without adding too much thickness to a low profile device. They work by evaporating water to steam, which transfers heat away from a heat source to the cooler regions of the chamber. This means that to simulate a vapor chamber correctly it would require simulating phase changes and rapid mass flows in very thin volume. This would consume a lot of computing time, which makes it unusable in detailed simulation in the system level models. Therefore, a simpler model has to be developed. A few of these exist, but they were considered to be too complex for the current application. The goal of this thesis was to develop a behavioral model, which would model the vapor chamber as one domain in the CFD simulation model.

Experimental data was taken as the basis of the behavioral model. The measurements were done with a 0.6 mm vapor chamber and a 3 mm copper reference sample. The experimental setup was replicated into a commercial CFD simulation software and the model was tuned to match with the calibration sample. Then, using the tuned model, the thin vapor chamber was simulated by assuming various thermal conductivity values.

Data from the simulations were compared to the experiments by using RMSE minimization. It produced a function that described how the vapor chamber's effective conductivity changes with temperature. To use the algorithm built into the CFD software, a linear approximation was applied to the function. The linearization provided parameters that enabled to create a temperature dependent material model that was used in the one cuboid behavioral model of the vapor chamber.

TIIVISTELMÄ

LAURI NIITTYMÄKI: Joustava höyrykammion simulointimalli mobiililaitteiden lämpösimulaatioihin
Tampereen teknillinen yliopisto
Diplomityö, 47 sivua
Lokakuu 2016
Materiaalitekniikan diplomi-insinöörin tutkinto-ohjelma
Pääaine: Materiaalitutkimus
Tarkastaja: professori Veli-Tapani Kuokkala

Avainsanat: höyrykammio, käyttäytymismalli, lämmönhallinta, lämmön levytys, simulointi, CFD, mobiililaite

Kasvava laskentateho kannettavissa laitteissa nostaa myös niiden sisällä olevan elektroniikan tuottamaa lämpökuormaa. Laitteen suunnitteluvaiheessa lämmöntuotto pitää ottaa huomioon, jotta laitetta on turvallista käyttää. Simulointi on yksi työkaluista, joita käytetään suunnitteluvaiheessa löytämään paras ratkaisu. Se mahdollistaa erilaisten ratkaisujen kokeilun, ja ohjelmiston optimointityökalut auttavat parhaan ratkaisun löytämisessä.

Höyrykammiot ovat ohuita levyjä, jotka voivat levittää erittäin suuren määrän lämpöä suurelle pinta-alalle ilman, että laitteet paksuutta pitää muuttaa. Niiden toiminta perustuu kammion sisällä olevaan höyryyn, joka kuljettaa lämmön pois kuumalta alueelta. Tästä johtuen niiden yksityiskohtainen simulointi vaatii faasimuutosten ja nopeiden massavirtojen laskentaa ohuessa tilassa. Tämä ei ole mahdollista monimutkaisten järjestelmätason simulointimallien kanssa, sillä niiden ratkaiseminen kestäisi liian kauan. Näin ollen tähän tarkoitukseen tarvitaan yksinkertaisempi malli. Kirjallisuudesta löytyy yksinkertaistettuja malleja, mutta niiden tarjoama hyöty ei ole riittävä. Tämän työn tavoite oli kehittää yksinkertainen käyttäytymismalli, jolla höyrykammiota voidaan simuloida käyttämällä vain yhtä kappaletta.

Mittausdata otettiin mallin lähtökohdaksi. Kokeissa käytettiin 0,6 mm paksua höyrykammiota ja 3 mm kuparilevyä referenssinäytteenä. Koejärjestely kopioitiin mahdollisimman tarkasti simulointiohjelmistoon, joka kalibroitiin referenssinäytteen tuloksilla. Kokeiden ja simulointien pohjalta jokaiselle lämmitysteholle muodostettiin virhefunktio. Tämän avulle höyrykammion käyttäytyminen voitiin karakterisoida.

Kuten oli odotettua, höyrykammion efektiivisen johtavuuden todettiin nousevan, kun lämmitysteho kasvoi. Simulointien yhteydessä huomattiin myös, että levyn lämmönlevitysvastus lähestyy minimiarvoa, kun lämmön johtavuutta nostetaan. Simuloinneista ja kokeista saatu data yhdistettiin laskemalla RMS virhe. Tästä saatiin funktio, joka kuvaa höyrykammion efektiivisen lämmönjohtavuuden muutoksia lämpötilan funktiona. Koska käytössä olleeseen CFD ohjelmistoon voitiin asettaa vain lineaarisia riippuvuuksia, jouduttiin tekemään lineaarinen approksimointi. Tämän lopputuloksena olivat tarvittavat parametrit lämpötilariippuvan materiaalimallin luomiseen, jota voidaan käyttää käyttäytymismallissa.

PREFACE

The thesis was written for the Department of Materials Science at Tampere University of Technology and Intel Finland OY.

I started working at Intel in summer 2015 as a trainee. The work was very interesting and I was glad that I got an opportunity to continue working at Intel with this thesis. For this I want to thank Timo Herranen for giving me this opportunity and letting me to work in such a great environment. My advisor was PhD Cathy Biber at Intel, who guided me through this work. I want to express my sincere gratitude to her as she sacrificed so much time to help me forward. I also want to thank my examiner Prof. Veli-Tapani Kuokkala. He provided helpful feedback and guidance during the writing process.

I want to thank my parents for supporting me during these years of studying, as well as my partner Anna for all the advice she has given to me. She has also helped me to find the motivation to complete this work.

Finally, I want to thank all the friends I have met in TEA-club and Nääspeksi during my time at TUT.

Tampere, 26.10.2016

Lauri Niittymäki

CONTENTS

1. INTRODUCTION 1
2. THEORY 4
2.1 CFD simulation 4
2.2 Vapor chamber 5
2.2.1 Working principle 5
2.2.2 Structure 7
2.2.3 Operation limits 9
2.2.4 Materials 14
2.3 Vapor chamber simulation 20
3. MEASUREMENTS AND SIMULATIONS 23
3.1 Experiment setup 23
3.2 Simulation setup 26
4. RESULTS AND CHARACTERIZATION 29
4.1 Results from the experiments 29
4.2 Results from the simulation 31
4.3 Behavioral model of the vapor chamber 35
4.4 Applying the behavioral model 36
5. CONCLUSIONS 40
REFERENCES 44

LIST OF SYMBOLS AND ABBREVIATIONS

SoC	System on a chip
PC	Personal computer
CFD	Computational fluid dynamics
TIM	Thermal interface material
CPU	Central processing unit
CTS	Coefficient of thermal spreading
TTV	Thermal test vehicle
PCB	Printed circuit board
TC	Thermocouple
RMSE	Root mean square error

1. INTRODUCTION

The computing power in mobile devices is constantly increasing as people want to get more out of their devices. Applications like live video streaming, gaming, real time editing of photos and two-way video calls are getting more and more popular. At the same time required resolution and number of calculations done behind the scenes are increasing. In addition, consumers expect devices to be thinner, lighter and made of high quality materials like anodized aluminum and glass. Component manufacturers have been reacting to this need for more computing power and have been developing more powerful chips for hand held devices. More and more transistors and computing units or cores are squeezed into a single package. This means that more heat is generated by the system on a chip (SoC) and other components.

Increasing heat loads are a huge problem in small devices like tablets or smartphones, because the ways to dissipate heat are more limited than in a larger a PC. In these applications, good thermal management is particularly important. Under heavy workload devices can easily overheat, which can cause damage to the components or feel uncomfortable to the user. Therefore, new ways to manage heat loads must be discovered. Simulation is a quick and cheap method to test different concepts and designs before any prototypes are made. Reliable simulation models are needed to accurately represent heat flow inside a system.

One way to increase the heat flow in a small device is to spread heat by using highly conductive materials. Traditionally this is done by attaching thin aluminum or copper sheets over a heat source and spread heat to the battery or other structures. A problem with this solution is that high temperatures can damage the battery or shorten its lifespan. Also, heat flow in mechanical structures tends cause local hot spots if the thermal conductivities are low. Such hot spots on the outer surface of the device may be uncomfortable or even dangerous to the user holding the device. One way to reduce hot spots on the surface is to leave air gaps between the cover and the hot area. This however, means that the heat must flow some other place where it can be dissipated safely.

Since devices are getting thinner, there is not much space left for thermal solutions to fit in. Some manufacturers have started to use heat pipes to transfer heat to cooler areas. Mainly, this technique is applied to route heat away from the main circuit board to the mid-frame, which is often made of a metallic material. Magnesium, aluminum and steel are the most common materials for this. But some manufacturers, for example Apple, favor architecture where there is no mid frame to achieve thinner constructions. Heat will

spread through the circuit board and display support structures. The risk is that the temperature on the display glass will exceed the comfort limit.

One potential technology for better heat spreading is vapor chambers since they offer very good heat spreading properties in very thin form factor. Manufacturers have now managed to produce thin vapor chambers suitable for thin devices. Even vapor chambers less than 0.5 mm thick exist.

Like heat pipes, vapor chambers combine heat conduction and phase change to transport heat away from a heat source. They are constructed from two copper sheets, which have an internal geometry featuring a wick and a vapor space. The wick transports water to the heated area, and the vapor space allows water steam to spread to the cooler parts of the vapor chamber. Water condenses back into liquid and the porous wick brings it back to the heater with capillary action. A more detailed description of vapor chamber is presented in the theory section.

Combination of phase change and rapid mass flow inside the vapor chamber makes it complicated to simulate with a computational fluid dynamics or CFD software. Simplified models have been created to resolve this problem. [1,2] However, most of them divide the vapor chamber into functional sections like the wall, the wick and the vapor space. This creates a model that can represent well the mathematical properties of the vapor chamber, but sometimes these can be hard to integrate into existing software. Also, modifications might be impossible if the person who made the model or integration is not available, or if internal construction details of the vapor chamber are unknown.

To simulate a vapor chamber in an entire system, a much simpler model has to be used. Since system level models take into account everything from heat generation by a component to convection generated by the heat on the surface of the system, they will take some time to solve. During a product development cycle, time used to solve the model is not productive, and therefore simpler models are preferred. Consequently, the goal of this work is to find a model that represents well the vapor chamber's spreading ability and scales to changes like size thickness and heat input. To achieve maximum simplicity, the aim is to use one simulation domain to model the geometry and the behavior of the vapor chamber. Because no software integration or mathematical modelling is required, this method should be easier to understand and modify by persons who will work with it in the future.

The proposed model would help engineers in the design phase of a product to test different constructions, geometries, and heat loads more quickly as there is no need to create an individual model for every variation of a vapor chamber. Because models are often based on measurements that are made with prototypes, a more robust model would reduce the number of prototypes required. Consequently, also the cost would be reduced since prototypes are often quite expensive.

A second objective of this work is to develop a modeling method that can characterize a vapor chamber easily over a range of likely application parameters. In this work only heat input is covered, since during operation it is the only parameter that changes.

2. THEORY

In this section, basic theory of computational fluid dynamics and vapor chambers is covered. First a quick introduction to CFD is presented and its usefulness for the electronics industry is discussed. Then the working principle of vapor chambers, structure and commonly used materials are described. The last part will introduce methods to model vapor chambers.

2.1 CFD simulation

Computational fluid dynamics (CFD) is a numerical method to solve the equations of fluid motion, heat flow, and thermal radiation subject to boundary conditions. It is widely used for example in aerodynamics, weather modeling, and electronics. The basic idea behind CFD is from the early 1920's, but development in computing power during the 80's and the 90's made possible to utilize its full power. [3] Nowadays there are numerous commercially available CFD codes, some of which target specific applications, including electronics cooling.

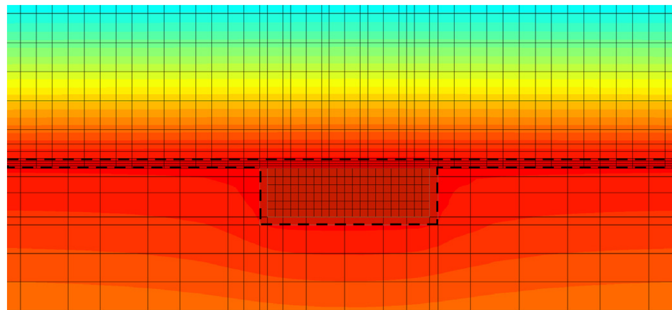

Figure 1. *Illustration of a simulation model, which is divided into grid cells (continuous lines). The dashed line shows the solid part of the model. Colors represent temperature.*

Fluid motion and heat transfer are governed by a set of partial non-linear differential equations known as the Navier-Stokes equations. These apply the laws of physics to conservation of mass, momentum and energy. It has long been known that these cannot be solved analytically except in very limited situations, which means that other ways to solve them had to be developed. In CFD this is done by dividing the continuous domain into finite domains called grid cells. For each grid cell a set of algebraic equations can be formed so that the solution can be calculated at the center of each grid cell. Figure 1 shows how a model is gridded. Areas that are more interesting or have high gradient are gridded

denser. Here, the solid parts like the heater and the spreader have smaller grid cells to make the calculations more accurate. The whole set of equations is then solved iteratively with the boundary conditions. [4]

In the electronics industry the main focus of the CFD simulation effort is the concern that temperature of all components has to be kept under their thermal limits defined by the manufacturer. Also for hand held devices, certain surface temperature limits have to be met to ensure user comfort and safety. Consequently, in hand held electronics, the main attention when doing a CFD simulation is not on how fluids are behaving and interacting with each other but rather on modeling heat transfers inside and adjacent to the system. However, the fluid behavior on the exterior surfaces affects the internal behavior and vice versa, so that the exterior and the interior analysis must be performed together. This is so-called “conjugate” heat transfer problem. [5]

To make this more reliable and effective, most CFD software offer a library of ready-made components, which can be modified with parameters to make them fit a certain design. It makes the design process simpler as the thermal engineer does not need to take the time to model every single component from basic primitives. Such components are fans, circuits board, heat sinks, and electronic components. These components speed the modeling process for the engineer. Also included in most CFD products are some degree of extra complexity like thermal radiation, solar load, variable properties, and so on. The use of these approaches to make good design decisions is by now well established, with many reputable vendors and various application domains. [6,7]

2.2 Vapor chamber

The basic idea behind heat pipes and vapor chambers was patented independently by Richard Gaugler in 1942 [8] and George Grover in 1963 [9]. They both suggested that heat could be transferred away from a heat source in a sealed tube by vapor. The vapor will condense back to liquid when it reached cooler region. In addition, the liquid could be returned to the heat source without a pump or gravity by using the capillary action. Nowadays heat pipes and vapor chamber are used in a wide range of applications from consumer electronics to spacecraft.

2.2.1 Working principle

Liquids like water have been long used as coolant since they are easy to pump from a heat source to a remote radiator and they usually have a high heat capacity. In this way, a lot of heat can be transferred away much more efficiently than with solid conductors. In order to transfer heat from places which cannot be cooled directly, for example with a heat sink, liquid cooling provides superior cooling performance compared to other cooling solutions. In the cooling consumer electronics, it is used in high power systems like enthusiast grade gaming systems, but in professional systems it is considered to be too unreliable.

This is because liquid cooling often requires active components like pumps to work, which are not that reliable. Furthermore, in mobile systems active liquid cooling is not feasible, since due to the volume and weight of water, the pump and radiator cannot be fitted into thin device system. As a result, heat pipes and vapor chambers are ideal in heat transfer and heat spreading for small systems. Natural capillary action takes care of pumping so there is no need to include a separate pump. The wick also handles pumping more reliably than a mechanical pump. [10]

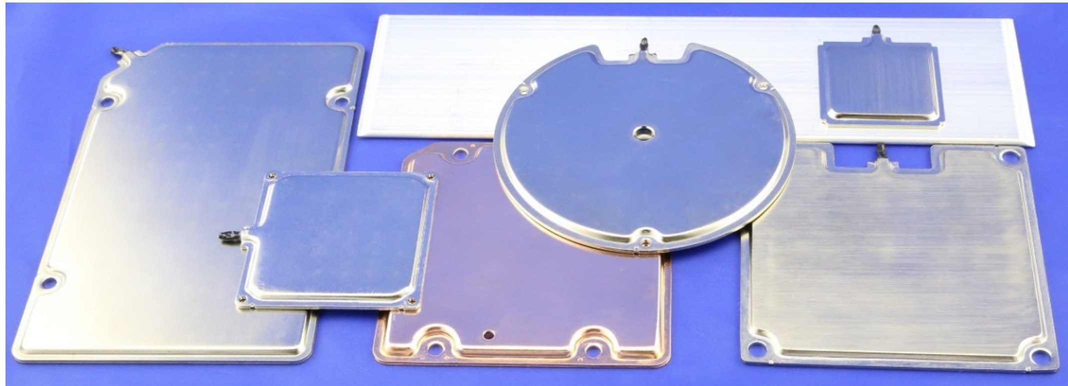

Figure 2. *Different vapor chambers. [11]*

Vapor chambers are two phase heat spreading devices closely related to heat pipes. They share the same working principle and the basic theory can be applied to both of them. The main difference is that while heat pipes are long pipes, vapor chambers are often more like plates. Some examples can be seen in Figure 2. Consequently, unlike heat pipes that tend to transfer heat from one narrow location to another, vapor chambers can spread heat to a wider area. The wider area gives better thermal dissipation performance and temperature uniformity to a system. This helps to better transfer heat to a heat sink or in the case of a mobile device, to the cover of the device. Uniform heat distribution is essential to achieve better user experience and better performance without thermal throttling, and also to increase the dissipation capability of the device while maintaining user comfort temperature limits on the cover.

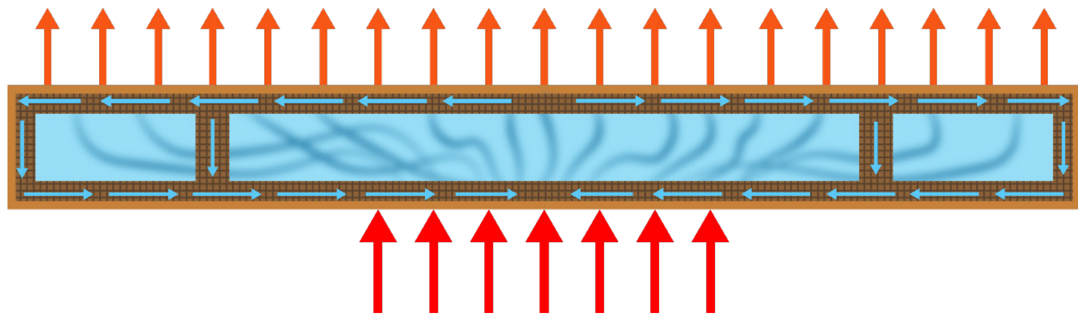

Figure 3. *Heat and mass flow inside a vapor chamber. After: [1]*

Both the heat pipe and the vapor chamber work through a phase change process, which is driven by a heat load. The wall of the vapor chamber is thermally connected to a heat source, often with a thermal interface material (TIM). Heat is conducted through the wall to the wick and then to the working fluid. It evaporates from the wick to the vapor space. This vapor space is typically below the atmospheric pressure. The vapor travels from near the heat source to a cooler area in the spreading device and condenses back to liquid. The wick absorbs the working fluid back in, and capillary action draws it back to the evaporator. An illustration of this process is shown in Figure 3. Because the vapor condensation area can be anywhere that the temperature is lower, the temperature differences are minimized. This is further amplified by the fact that higher power drives vapor farther from the heat source as it expands into a larger cooler region. With these processes the vapor chamber can achieve an order of magnitude or greater effective conductivity than copper or other solid conductors. [10,12]

Vapor chambers and heat pipes can react to heat load changes very quickly. This is because the thermal mass of the vapor chamber is very low and the steady state conditions are reached relatively quickly. It is very useful especially in mobile applications, as for example live video streaming or gaming can cause rapid changes in heat loads. Also of practical importance is that with proper design, both heat pipes and vapor chambers are not significantly affected by gravity. [13]

2.2.2 Structure

The vapor chamber's structure is similar to that of most heat pipes. The biggest difference is that the vapor chambers are flat plates with big condenser area. The vapor space is between these two and vapor motion is mostly perpendicular to the evaporator. [14] In addition, vapor chambers can be used to cool multiple heat sources to transfer the heat to a common heatsink. [15,12]

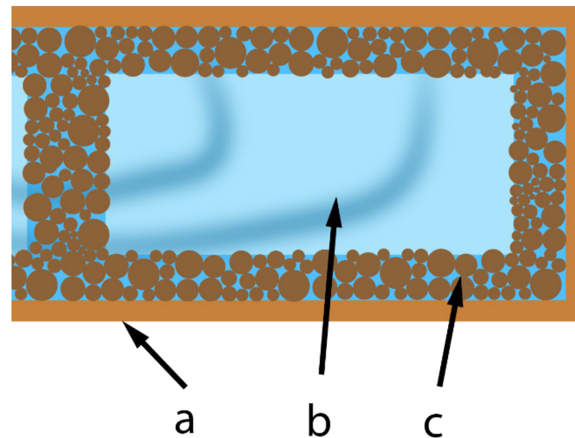

Figure 4. *Vapor chamber structure a) wall b) vapor space c) sintered wick with working fluid*

The basic structure of a vapor chamber is shown in Figure 4. The outmost layer of the vapor chamber is the wall. It is made of a solid material, usually copper, that is formed and cut to the right shape. The wall conducts and spreads heat from the heat source to the wick. It is important that the wall has sufficient thermal conductivity so that temperature on the heater stays low. As the vapor chamber has a near vacuum atmosphere inside, the wall also has to be completely sealed and it has to stay that way during its whole lifetime. With copper, proper sealing is done by crimping the filling tube and by cold welding it permanently. Other materials can be hot welded to melt the filling tube. [12]

The working fluid is charged into the vapor chamber during manufacturing through the filling tube. The working fluid type and quantity depend on the application, temperature range, and wick type.

The working fluid is incorporated into the wick. The wick can be a separate component, which is attached to the wall or it can be grooves that are part of the wall. The wick has an essential role in the vapor chamber because it circulates the working fluid inside the vapor chamber. In heat pipes, the wick is only on the wall, but as the vapor chamber needs more structural integrity, there are also spacers that are made from the same material as the wick. These also act as extra channels for the working fluid to travel more quickly back to the condenser area.

Many types of wicks exist, ranging from sintered powders to felts. In order to circulate the working fluid inside the vapor chamber, the wick has to be compatible with the working fluid. The wick has to be wetted completely by the working fluid to ensure proper capillary action. In some vapor chambers, the wick is only placed on the evaporator side and the condenser is left without it. Liquid working fluid drips back to the evaporator by gravity, but this will make the vapor chamber more sensitive to orientation. [16]

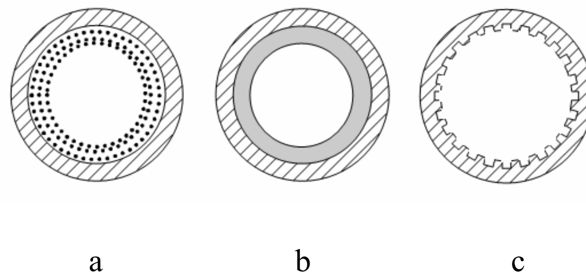

a b c

Figure 5. *Different wick types. 1)net, 2) sintered, 3) open channel or grooved [17]*

Three basic wick structures are illustrated in Figure 5. Net or mesh wicks are constructed of individual wires like fabric, which forms sharp corners and small channels and creates capillary force with the working fluid. The magnitude of the force can be controlled by wire diameter and number of mesh layers. More layers or bigger wire diameter will result in better wick performance. [18]

Sintered wicks are made of small grains that are heated so that they fuse together. This forms tiny channels that can provide a big capillary force. They also keep the working fluid inside so that it will not spill into the vapor space. However, small structures can be easily clogged by small bubbles. This can happen very easily in the evaporator section and can lead to dry out. [17]

In a micro-grooved wick structure, vaporization and condensation processes create curvature difference on the fluid surface. Since in the hot end of the heat pipe the fluid is vaporizing from the groove, it leaves a void behind before more fluid can flow into the hole. In the cold end, the condensation process causes grooves to be more flooded and here the surface of the working fluid is less curved that in the hot end. This drives the fluid motion in the grooves. [10] Open channels like grooved wicks will not be clogged so easily. In this structure, the channels are much bigger and open so that the bubbles can travel to the vapor space easier. However, there is a risk that also the working fluid can leave the channel before it reaches to evaporator. It can then be caught by the fast moving vapor and that way lower the overall performance of the vapor chamber. [17]

2.2.3 Operation limits

Since heat pipes and vapor chambers are based on mass flow, they are both limited by the physics which limits this motion. When the motion is limited, these devices will lose their capability to transfer heat properly. This will often lead to the formation of hot spots, which can lead to damage to the device that is being cooled. In electronics, multiple layers of protection are built into devices like CPUs to prevent damage in this kind of situation.

Consequently, the device is shut down before any damage can happen. After the device and the thermal solution have been cooled down, heat pipes and vapor chambers can recover the overheating and return to normal operation.

A vapor chamber is not always the right solution since a purely conductive spreader like copper, aluminum, or graphite may conduct heat better through its thickness than a vapor chamber. This is a result of the structure of the vapor chamber, as there are low conductivity components inside it and in that way copper may work better, if the heat is spread to a small area. However, as the spreader size increases, conduction in the solid is much less efficient than heat transport by vapor. The exact crossover point depends on the structure of the vapor chamber. [1]

According to Phaser [19], the vapor chamber's capability to transfer heat is limited by two factors: the heat transport capacity and the heat carrying capacity. The first one is ruled by the overall thermal resistance of the vapor chamber components and the temperature difference between ambient and the evaporator. The wick contributes the most to this as it has the lowest thermal conductivity. Consequently, if the thickness of the wick is reduced, the heat transport capacity will be increased. Equation 1 shows how the heat transport capacity is affected by these variables in a heat pipe.

$$Q_{transport} = \frac{\Delta T}{\frac{t_w}{k_w A_{evap}} + \theta_{adiabatic} + \frac{t_w}{k_w A_{cond}} + \theta_{hs}} \tag{1}$$

Here ΔT is the temperature difference between the evaporator and the condenser, t_w is the thickness of the wick, k_w is the wick conductivity, A_{evap} the area of the evaporator and A_{cond} the area of the condenser. θ_{hs} and $\theta_{adiabatic}$ are the thermal resistances for the heat sink attached to the vapor chamber and for the vapor space between the evaporator and the condenser. [19]

The capillary limit of the wick is the most dominant limiter in a vapor chamber. It also defines the heat carrying capacity of the vapor chamber. [13] When the evaporation rate exceeds the rate of the fluid flow in the wick, the evaporator starts to dry out. This leads to a dramatic temperature rise in this vaporization section and hence also in the heat source. This limit depends on the wick type and the cross-section area of it. Materials also affect greatly this factor since different material selections yield a different interface between the wick and the working fluid. [20] In equation 2 one can see that the thickness of the wick has an opposite effect on the carrying capacity of a heat pipe than on the transport capacity. If the wick is made thicker, the carrying capacity is increased. [16]

$$Q_{carry} = \left[\frac{\rho_l \sigma_l L}{\mu_l}\right] \left[\frac{2\pi C t_w r_w}{l}\right] \left[\frac{2}{r_e} - \frac{\rho_l g l}{\sigma_l} \sin \phi\right] \tag{2}$$

Here ρ_l is the density of the working fluid, σ_l the surface tension of the working fluid, L the latent heat of vaporization, μ_l the viscosity of the working fluid, C the permeability of the wick, t_w the thickness of the wick, r_w the average radius of the wick, l the length of the heat pipe, r_e the effective radius of the wick pore, g the gravitational acceleration and ϕ the angle from the horizontal plane to the heat pipe. If capillary force cannot pull the working fluid fast enough, the heat pipe or the vapor chamber will dry out. [13,19]

Equations 1 and 2 show that the wick thickness has an opposite effect on the vapor chamber's effective conductivity. This is further illustrated in Figure 6, which shows that the heat transfer capacity and the heat carrying capacity will cross at the point where the effective conductivity reaches its maximum value.

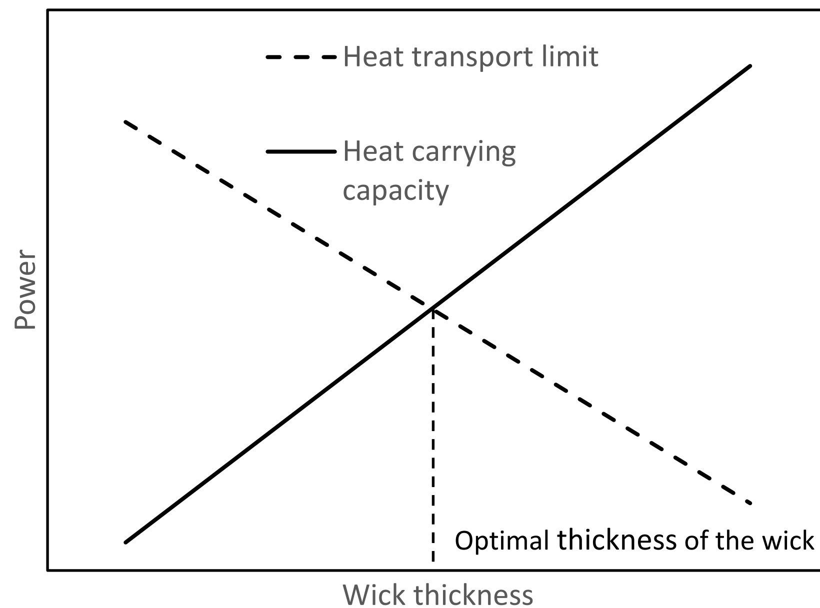

Figure 6. *Effect of power and wick thickness on the vapor chamber's capability to spread heat. After: [19]*

One can see from the picture and the equations that the thickness and the heat sink's thermal performance have the biggest contribution to the maximum performance of a vapor chamber. The heat sink in the case of a mobile device can be for example the back cover of the device. This means that these limitations have to be taken into account during the design phase of the device. For example, an aluminum back cover can spread and conduct heat out from the device much better than a plastic back cover, but on the other hand the perception of temperature when touched means that its temperature limit is lower.

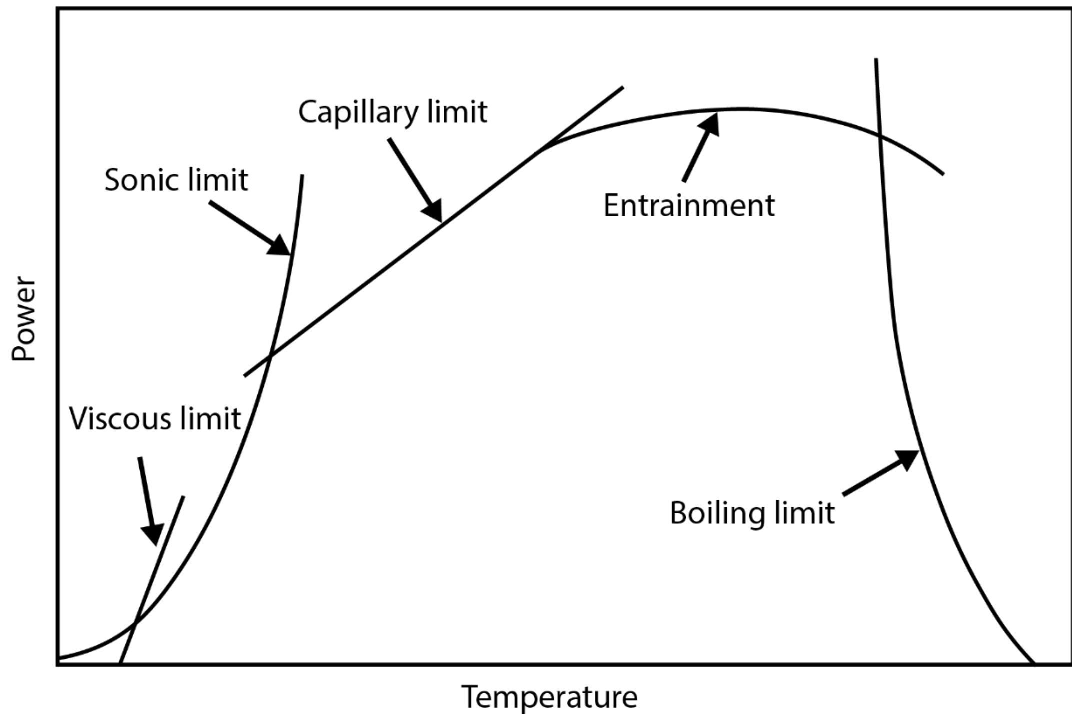

Figure 7. *Approximate illustration of the operation limits of heat pipes. [10]*

Figure 7 shows theoretical operational limits of heat pipes. The same physical rules apply also to the vapor chambers. As mentioned earlier, the capillary limit is the most common phenomenon that limits the low temperature heat pipe performance. It happens when the wick cannot pump enough liquid to the evaporator section. In this situation, the sum of the liquid and the vapor pressure drop is more than the capillary pressure. Exceeding the capillary limit will always lead to dry out and a sudden increase in the evaporator wall temperature. [21]

If heat pipes or vapor chambers are subjected to low temperatures, the viscosity of the working fluid might increase so much that it will not flow inside the wick. This is called the viscous limit and it defines the lowest operating temperature. The most extreme case is when the working fluid is in a frozen state. This situation can occur when the vapor chamber is below its operation limit when the device is turned off or just starting up. Before the vapor chamber can operate, the working fluid has to be melted in order to get the natural capillary force working. [17] The viscous limit is a bigger problem in heat pipes that use liquid metal as a working fluid. Applying a high power to a heat pipe, which is below the viscous limit, will lead to overheating and local dry out. [21]

A sonic limit can occur at low temperatures when the vapor pressure is small but heat is applied to the evaporator. This will cause rapid evaporation of the working fluid, which in turn creates high flow rates between the wick and the vapor space. Since the wick does

not have nozzle type features to make this flow stricter, speed of the vapor flow cannot be over the speed of sound. The same limit is reached if the vapor velocity is high in the vapor space. [22]

When a heat pipe or a vapor chamber is operating at high power and high temperature conditions, the entrainment limits performance of the system. Vapor and liquid that are flowing with high speed in opposite directions can interact at the vapor-fluid interface so that it comes unstable. This can cause droplets of the liquid to be caught by the fast moving vapor. If entrainment increases too much, it will lead to flooding of the condenser which will prevent both the condensing and the liquid motion within the wick. Since vapor chambers tend to have large condenser and vapor space, this is not a big problem in the vapor chamber. [23]

When the vapor chamber wall temperature increases too high, the working fluid starts to boil inside the wick. At this point, the boiling limit of the heat pipe or the vapor chamber has been reached. It can result in a situation where the wick is not anymore wetted by the working fluid. The cooling effect is then lost and the wall temperature will further increase and a hot spot will form. To recover from boiling, heat input has to be decreased so low that boiling stops and normal capillary driven liquid flow continues. In electronics, the recovery will happen automatically when the device overheats and is forced to throttle SoC down to lower heat output. [21]

In some cases, non-condensable gas can accumulate into a heat pipe. It will render part of the condenser unusable since it blocks part of the volume in the vapor space. This problem can be easily prevented during manufacturing by evacuating the heat pipe or the vapor chamber properly before sealing. Gas can also be generated through a chemical reaction between the materials inside the system. This part will be covered in the next section. [21]

To ensure that the operation limits are not reached during normal operation, the design process of a vapor chamber is handled by the supplier. They have the required specialists and equipment to properly manufacture working vapor chambers for each application. They have to take into account multiple variables to suit the intended application. These are, for example, the heat input density, the operating temperature, gravity and the thickness. When designing a heat pipe or a vapor chamber, the most important factor to consider is to define how much power the vapor chamber has to transfer. Depending on the application, the heat pipes and vapor chambers can transfer anything from a few watts to more than a kilowatt. [10] The supplier also has to select what kind of internal structure will be used. For the wick, sintered structure is the most common choice. The supplier has to be also capable of manufacturing vapor chambers that meet the desired design intentions. Essential is that the vapor chamber is charged with just a right amount of working fluid and that all non-condensable gas is evacuated from the vapor chamber. [24,25]

2.2.4 Materials

Understanding how materials behave and react with each other in different temperatures and environments is very important when selecting materials for a vapor chamber or a heat pipe. Conditions are extremely different on the opposite sides of the wall, and temperature changes can be huge between the non-operational and operational states. Therefore, materials that can handle these conditions and do not react with other materials present must be selected.

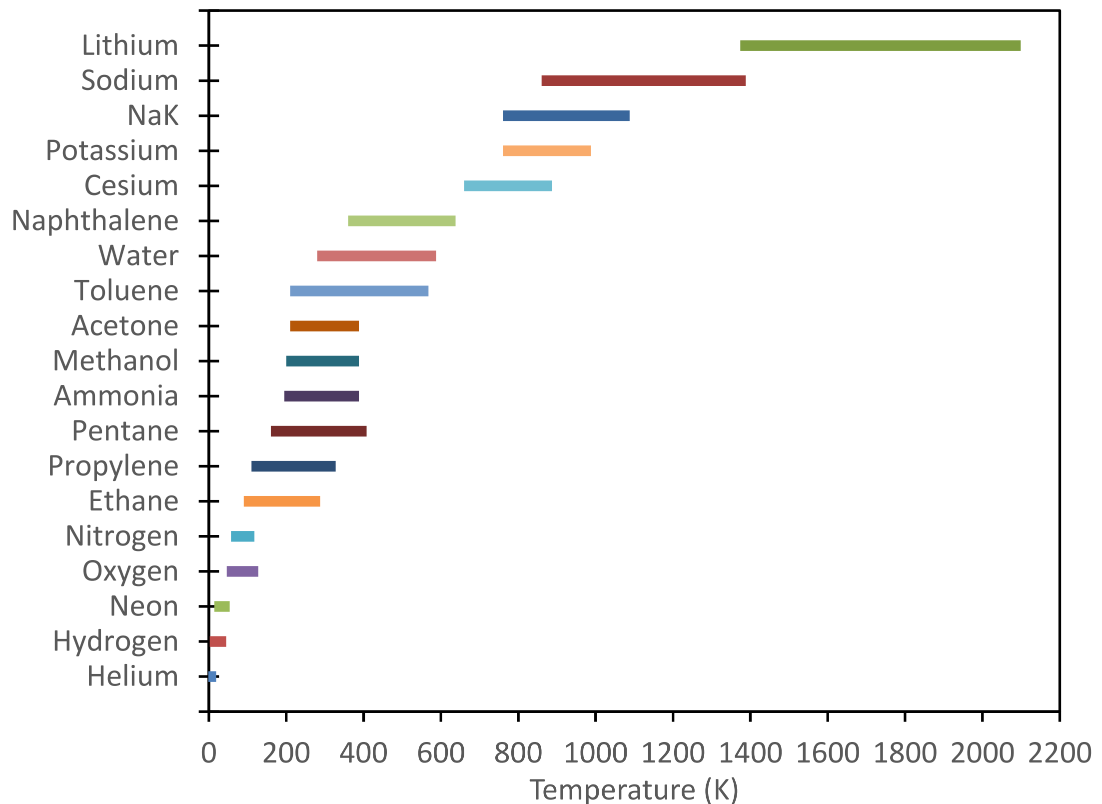

Figure 8. *List of working fluids and their operating temperatures. [12,27]*

The working fluid dictates the operating temperature range of a heat pipe. This means that it has to be selected so that it can perform well in the intended conditions of use. The lower limit of the operating range is the melting point of the working fluid and the upper limit is the capillary limit or the boiling limit. In most cases, the most corrosive or reactive material in a heat pipe is the working fluid. Therefore, the other materials can be selected only after the working fluid is decided. Many different choices are available to be used as the working fluid, but some options are very corrosive or poisonous. [12] In Figure 8 some of the possible working fluids are listed with corresponding operating temperatures.

It is easy to see that there is a very wide range of working fluids to suit different operating temperatures. [26]

The working fluid has to be selected well to maximize the heat transfer. As mentioned earlier, the working fluid handles the most significant portion of the heat transfer in a heat pipe and a vapor chamber. It has to have certain properties so that good heat transfer capability is ensured. To achieve this, the working fluid should have high surface tension, high thermal conductivity, good wettability of the wick and the wall, low viscosity, and high latent heat of evaporation. High surface tension keeps the molecules in the liquid together, which helps to keep it flowing inside the wick even against gravity. The surface of the liquid acts as a stretched film, which is created by the attractive forces between the molecules. These forces vary with temperature and pressure, but changes are very small compared to the other forces in the system. [26]

The thermal conductivity of the working fluid has to be as high as possible. This helps to carry heat from the wall and the wick evenly into the working fluid. Also, when the liquid is in the wick, good thermal conductivity will reduce radial thermal gradient. It can help to minimize the risk of localized boiling at the interface between the wick and the wall. [26]

In order to have a good capillary force, the working fluid has to wet the wick and the wall completely. If the continuous fluid film is broken, then the flow will be disturbed and might lead to dry out. If this happens at the evaporator area, it might lead to local hot spots. The wettability can be controlled by selecting materials so that the solid materials, the wick and the wall, have a higher surface energy than the working fluid [28] and by ensuring that the solids are pure from impurities. [29] Also, the wick type and structure have to be suitable for a particular working fluid. For example, in a mesh wick with water working fluid, when the wire diameter is increased the capillary limit also increases. [18] High surface tension helps also to wet the wick and the wall. [26]

The performance of a heat pipe or a vapor chamber is greatly reduced if the working fluid cannot flow freely inside the wick. As a result, a low viscosity liquid is preferred. Low viscosity allows the liquid and the vapor to flow easily in the system, which drives the capillary limit to a higher level. Low viscosity also lowers the pressure drop in the wick. [26,28]

During vaporization, energy is needed to turn liquid into vapor. The energy is held by the vapor until it is turned back to liquid. [30] In heat pipes and vapor chambers high latent heat helps to move large amount of heat with minimal fluid flow inside the system. It can avoid entrainment and makes the performance better at the capillary limit. [12,26]

Other important properties for the working fluid are compatibility with the wick and the wall, thermal stability, and appropriate pressure over the operating temperature. [26] As said earlier in this section, other materials can be selected only when the operating limits

and the working fluid have been decided. Thus, the compatibility of the working fluid with the other components inside the system can be better ensured. If a bad material choice is made, the whole heat pipe or vapor chamber can fail quickly. Often this is caused by corrosion, gas generation, or choking of the wick by solid material.

Gas generation and deposits can also form in a heat pipe, if the working fluid is not chemically stable at high temperatures. Therefore, thermal stability is a very important property of the working fluid. Thermal stability means that the working fluid does not break down into its components during operation. [26] If breakdown happens, the mass of the working fluid is reduced over time and the combined gas and deposit generation will lead to failure.

A heat pipe or a vapor chamber is a tightly closed vessel that does not let gasses escape. This means that the pressure inside the system has to be between suitable values. Too low pressure will lead to high vapor velocities and entrainment. Too high pressure might damage the mechanical structure of the heat pipe, which could lead to the failure of the wall. After evacuation and during normal operation, the pressure is equal to the saturation pressure of the working fluid at the current temperature. [12,31]

The wick has a very important role in a heat pipe or a vapor chamber since it is responsible for circulating the working fluid. It has to have high surface energy so that the working fluid is going to wet it completely. [28] The wick also has to contain features that allow the capillary force to be as high as possible. In addition, a material which has high thermal conductivity is preferred, since the wick often has the lowest thermal conductivity in the system. For example, the condenser vapor releases its latent heat to the wick which has to conduct the heat to the wall. If the wick has too low thermal conductivity, the radial temperature gradient will be increased. [31]

Most metals provide high thermal conductivity and for that reason are often used as wick and wall materials. Heat is conducted through a material with electrons and lattice vibrations or phonons. In metals the electrons carry most of the heat, while in other materials the phonons are more dominant. This is due to fact that metals have lots of electrons that can move through the lattice and carry heat efficiently. [32]

The wall is the only component that is in contact with the outside environment. It has to be able to seal the heat pipe completely so that the working fluid stays in and that the outside atmosphere cannot travel into the system. In other words, the wall has to form an isolating container so that only heat can conduct through it.

High thermal conductivity is a very important feature of the wall. It keeps the radial thermal gradient as small as possible, which means that also the device to be cooled will be closer to ambient temperature. High conductivity also reduces hot spots as it will spread heat laterally. Hence, the evaporator area will also increase since heat not only goes

straight through but also spreads. At the condenser, high conductivity allows efficient heat transfer from the working fluid and the wick to a heat sink or the cover of a device.

The working fluid has to wet the wick and also the wall well. Otherwise it can cause excess friction and slow flow of the working fluid. Furthermore, in some vapor chambers, the wick is only on the evaporator side and good wettability is essential in order to get the working fluid to spread to the condenser. Similarly, in the case of a grooved wick, the wall has to keep up the capillary pressure, which requires good wettability.

To maintain the structural integrity, the wall material has to be also compatible with the working fluid and other materials in contact with it. Consequently, the wall has to be able to withstand the outside environment.

The vapor chambers and heat pipes have to have sufficient mechanical properties so that they can take loads during assembly and operation. The wall is responsible for providing this strength. Because of this, the wall material has to have good mechanical properties but at the same time low density. Low density will keep the mass of the vapor chamber low.

In electronics cooling, a cheap material that is easy to manufacture is preferred as the wall material. Manufacturing includes machining, forging and welding. Consequently, copper, aluminum and steel are very popular heat pipe wall materials. [12]

As discussed in the previous sections, materials which can be used in heat pipes and vapor chambers vary depending on the temperature range. The cold end of the spectrum are called cryogenic heat pipes operating from 4 to 200 K. At such low temperatures only noble gasses or hydrogen and oxygen can be used as the working fluid. Other materials have to be compatible with them. Low temperature heat pipes operate between 200 and 500 K and they are the most common. Here mostly materials that are compatible with water, ammonia and acetone can be used. When temperatures go beyond 500 K, the heat pipes are called high or super high temperature heat pipes. At these temperatures materials that can be used are more restricted. Since common wall materials like copper and aluminum are not usable at temperatures over 1000 K, other materials with a higher melting point have to be used. [33,34] In Table 1 some usable materials are listed with compatible working fluids.

Table 1. *Material compatibility*

Wall/wick material	***Compatible***	***Non-compatible***
Stainless Steel	Widely compatible	Water, Methanol
Copper	Methanol, Water, Nickel, Acetone	Ammonia, Cesium, Potassium, NaK
Titanium	Helium, Toluene, Water, Cesium	Potassium, Sodium, Ammonia, Methanol
Aluminum	Oxygen, Nitrogen, Ethanol, Propylene, Pentane, Ammonia, Acetone, Toluene, Naphthalene	Methanol, Water
Nickel	Propylene, Ammonia, Water, Acetone, Methanol	NaK
Copper-nickel	Toluene, Naphthalene	Cesium
Monel	Water	Cesium, Potassium, NaK
Steel	Ammonia	Water
Inconel	Potassium, Potassium	Water
Tungsten	Lithium	
Molybdenum	Lithium	
Silica	Methanol, Acetone,	Water

As said previously, copper is the most commonly used material in heat pipes and vapor chambers. This is because it has high thermal conductivity and it is easy to manufacture. It is also compatible with water, which makes it a perfect choice in electronics cooling. During endurance tests it has been noted that copper water heat pipes can operate long times without corrosion or gas generation. [35] However, an oxide layer will form on its surface, which lowers the surface energy and hence the wettability. To avoid this, during manufacturing all surfaces that will be in contact with water have to be cleaned carefully and sealed from oxygen. [29] Copper has a melting point of 1084 °C so it cannot be used in high temperature heat pipes. [36]

Stainless steels offer a higher temperature limit than copper since they have a melting point of about 1500°C. As they are chemically stable, they have very good compatibility with most low temperature working fluids. They also offer good resistance to chemicals outside the heat pipe. Some grades are not compatible with water since gas generation has been observed. [37] However, stainless steel provides good properties and performance for very broad range of temperatures. [26] Although stainless steels have good compatibility and a wide temperature range, they have low thermal conductivity compared to aluminum and copper. This limits their use in electronics cooling where high conductivity is important [16]

Monel is a nickel and copper alloy that has good mechanical properties over a wide range of temperatures and a high resistance to corrosion, and is therefore suitable for use in

difficult conditions. It can be used as a heat pipe wall material with water as the working fluid. [26,38]

Some other special materials can also be used. For example, plastics have been considered as the wall material in low temperature applications. Polymers, however, tend to have low thermal conductivity, which makes them quite inefficient. In super high temperature applications, ceramic materials can be used. They also have low thermal conductivity but if temperatures are very high, ceramics offer a good alternative. [16]

Materials that can be used as the wick are very similar to the wall materials. Often the same material as the wall is used to avoid galvanic corrosion between the wick and the wall. As described earlier in this section, high surface energy is needed from the wick material since it will make the working fluid to wet the wick better. Similarly with the wall, copper is the most commonly used material. It can be powder that is sintered to form small channels, or it can be made to a mesh. High temperature heat pipes have to have materials that can retain their properties at high temperatures. Some other materials than metals have also been tested for these application. For example, glass fibers have been tested as the wick material, but it was noticed that quartz crystals tend to form into it blocking the fluid flow. [26]

From all possible working fluids, water is the most commonly used working fluid in heat pipes and vapor chambers. This is mainly because it is suitable to cooling electronics, which mostly operate between 25 – 100 °C. It is also an ideal working fluid as it has high latent heat of evaporation and high surface tension. The corrosive nature of water limits the materials that can be used with it. For example, aluminum and steels are incompatible with water. Oxidation of the metal will cause gas generation and corrosion to the solid structures. [26]

Ammonia can be used in low temperature applications as the working fluid. With aluminum heat pipes, it can be used in low temperature applications like in spacecraft. [39]. Ammonia can be used with steels and nickel metals in other applications as well. [26]

In high temperature applications, materials with a higher melting temperature have to be used. Common working fluids in these kinds of applications are potassium and sodium. The operation temperature for them are around 500 to 1000 °C. They can be used in stainless steel heat pipes. If temperatures rise above 1500 °C, tungsten heat pipes can be used. With them, lithium is used as the working fluid. [26] Other alkaline metals can be also used. They generally have high a latent heat of evaporation and high surface tension.

The biggest problems when selecting materials to heat pipes or vapor chambers are corrosion, gas generation, and solid material deposition in the wick. [16] Corrosion happens outside or inside of the heat pipe. The outside surface of the wall is in contact with ambi-

ent atmosphere. Most metals will form an oxide layer if there is oxide present in the atmosphere. The oxide layer will protect the metal from corrosion. However, if the atmosphere is alkaline, the oxide layer will be dissolved and corrosion will continue.

Chemical reactions inside the heat pipe or vapor chamber can generate gas. Often the gas is hydrogen from an oxidation reaction between the working fluid and the solid components. [31] This non-condensable gas will accumulate to the condenser section of the heat pipe. It will act as a barrier for the vapor and will block part of the condenser. Consequently, the performance of the heat pipe will be reduced since the vapor has a smaller area to condense. A non-condensable gas can be identified by a sharp temperature change at the gas vapor interface. [16]

In high temperature heat pipes, corrosion can happen if some components dissolve to the alkali metal working fluid. [34] It is most likely to cause mass transfer between the condenser and the evaporator. Deposition will accumulate to the hot end of the heat pipe, which leads to hot spots and blocking of the capillary inside the wick, stopping the fluid flow.

In the literature one can find some compatibility data to help to make correct material choices. Long term studies have been done on heat pipes to find suitable material combinations. [26,40] However, the heat pipe and vapor chamber manufacturers mostly carry their own tests to verify that all materials are compatible and that the system will operate without failure over its lifetime. [16]

2.3 Vapor chamber simulation

General purpose CFD software is capable of solving mass flows, phase changes, and capillary action in porous media, but it would require too much computing power to do this calculation during the product engineering cycle. For this reason, vapor chamber thermal models are often approximations and do not include the process happening inside the vapor chamber.

In the literature there are simulation methods where mass flows like vapor motion and liquid flow in the vapor chamber are excluded. This can be done with the knowledge that the vapor is the biggest contributor to heat transfer. The vapor is substituted with a domain that has very large thermal conductivity. [2,19,41] Thereby the model will become purely conduction based and will be much simpler to solve.

Although mass flow is excluded from the model, it is still needed to subdivide the vapor chamber into sections according to the structure. In principle, in this model there is a thin layer of copper wall on the top and the bottom. Adjacent to that there is a low conductivity section mimicking the wick structure that has low conductivity as it is not solid copper

but rather a porous material. The porous material could be for example a screen or a sintered powder. In the center of these layers there is a section that has very high thermal conductivity. This represents the vapor, which can move freely at sub-atmospheric pressures. One feature of this model is that there are adjacent cells that have orders of magnitude of difference in their thermal conductivity. Also notable is the fact that this method creates very thin grid cells for thin physical structures, but which are not adding much to the accuracy of the solution. A good agreement is achieved but the thin grid cells and the large number of cells required slow down the convergence of the total product thermal analysis. [1]

To make a simulation model more robust and flexible, it has to somehow take into account the physical processes happening without actually modeling them in detail. The model also has to produce good agreement with experimental results with different heat inputs, geometries and thicknesses of the vapor chamber. Also, a typical product has variable thermal profiles and boundary conditions. The simplest approximation is to use a single domain for the vapor chamber with a high value of thermal conductivity. This would make the model more robust and accurate, as it does not require small and very different domains adjacent to each other. However, this constant conductivity model does not adapt to variable power. The diffusion theory predicts that when the heat flow doubles, the temperature difference also doubles. Because of the internal mechanisms, vapor chambers and heat pipes do not show this dependence. For example, the vendor data shows that the temperature uniformity changed by only 10% when the heat was doubled. This shows that the conductivity of the vapor chamber is increasing as the temperature is increasing. [42] Experiments done by Wang et al. [43] also show this behavior.

The next level of approximation is to use thermal conductivity that depends on the power. However, in the discretization required by CFD, the power is not a boundary condition on every cell, only on the vapor chamber itself or even on a separately modeled heat source. Therefore, this idea must be implemented so that the thermal conductivity is temperature dependent. Phaser [19] has presented Equation 3 which describes the vapor's thermal conductivity as a function of temperature.

$$k_{vapor} = \frac{L^2 p_v \rho_v d_v^2}{12 R \mu_v T^2} \tag{3}$$

Here L is the latent heat of vaporization, p_v the pressure of the vapor, ρ_v the density of the vapor, d_v the thickness of the vapor space, R the gas constant, μ_v viscosity, and T the temperature. The density and pressure of the vapor are also temperature dependent and will rise with temperature. This causes the value of the equation to increase as temperature increases. Equation 3 is based on ideal gas and it also makes assumptions like that the

vapor flow is laminar and that evaporation and condensation happen perfectly. Therefore, some error is introduced in the calculations. Furthermore, Equation 3 cannot be used if the structure, internal pressure, and the working fluid parameters are unknown.

Chiriac et.al. [44] have defined a figure of merit for mobile devices that makes the comparison of different thermal solutions easier. It is called the coefficient of thermal spreading (CTS) and it is a dimensionless number that tells how even the temperature gradient is on the surface of the device.

$$CTS = \frac{T_{ave}-T_{amb}}{T_{max}-T_{min}} \tag{4}$$

Here T_{ave} is the average temperature on the surface of the device, T_{amb} the ambient temperature and T_{max} and T_{min} the maximum and minimum temperatures on the surface. In a perfect situation, T_{ave} and T_{max} are the same and the whole device is perfectly evenly warm.

3. MEASUREMENTS AND SIMULATIONS

Experimental data is needed to create a working simulation model. In this work, the data was used to calibrate the model and to validate that it will give good results. The experiments were done with multiple different vapor chambers, but only one was selected to be used in this work to maintain best relevance.

3.1 Experiment setup

Experimental data of the vapor chamber samples were gathered with a thermal test vehicle (TTV). It is a test solution that allows to test and measure different thermal solutions without using a real CPU package in a controlled environment. In this case, all experiments were done in a chamber, which is kept at 25 °C and shielded from room ventilation to get better control over air around the sample. The actual TTV is a heat source that can mimic a CPU package with wanted heat source configurations and power settings. The TTV is soldered to the PCB so that the connections between the heaters and the sensors are accessible through connection pads on the PCB. The electrical connection between the TTV and the PCB also ensures that some heat is conducted to the PCB as it would do in the real product. Figure 9 shows the whole test setup.

Figure 9. *Test setup in the isolating chamber*

The TTV is attached to the green circuit board and it is under the black copper heat spreader. All connections for the TTV are located on the right-hand side of the image. A big connector is soldered to the circuit board, which allows to connect to the heater and the thermocouples inside the TTV itself. The circuit board is held in upright orientation by the plexiglass plate, which has a hole made to it to allow free air flow around the experiment. The whole assembly is kept in place by a structure made of aluminum trusses. This is then placed on a plastic grid, which allows air to move freely to mimic conditions where the device is held in hand. In this scenario, the spreader will heat the air around it and the air starts to move up. As mentioned previously, the experimental setup is placed in a chamber made of plexiglass to seal it from all the forced convection present in the normal room.

The TTV is constructed of a heat source the can be accurately heated with electric current. The heating power was constantly controlled and measured by an external system to get accurate heat input. The electric current was measured with high accuracy shunt resistors and a data logging software. To cover the whole possible power range from a chip, power settings 1, 3, 5, 7, 8 and 9 W were used. All experiments were running so long that steady state was reached. In this case, well over 30 minutes.

To get a better thermal connection between the heater element and the heat spreader, soft silicone based thermal interface material (TIM) was placed between them. Pressure was applied with clamps to help minimize air in the interface, which could introduce excess thermal resistance to the system. The applied pressure was measured for each experiment with a load cell attached to an acrylic block. These blocks were used on both sides of the stack to spread the pressing force evcnly over the heating element. It also thermally insulated the heat spreader and the TTV from the rest of the setup.

Thermocouples (TC) used in the experiments were first tested to ensure that they give consistent values. For this, all 14 thermocouples were attached to a vapor chamber with Kapton tape. The setup was in controlled environment with temperature set at 35 °C. There was not additional heater attached to the system. The measurement ran for 218 minutes, and a data point was recorded every 2 seconds. Then an average value for each time was calculated and each measurement point was compared to that. Last, the deviation from the average value was calculated for each thermocouple. Overall, the maximum difference was 0,125 °C.

The thermocouples were attached to both front and back surfaces of the heat spreader with thermal grease and Kapton tape. On the front surface the TCs where placed near the extreme corners and along the center line. This the way temperature distribution could be captured over the surface of the heat spreader. In addition, one thermocouple was located near the TTV on the back surface of the heat spreader. This allowed to measure temperatures near the evaporator. The TTV had its own built-in thermocouples, one of which was used. The thermocouple locations are shown in Figure 10.

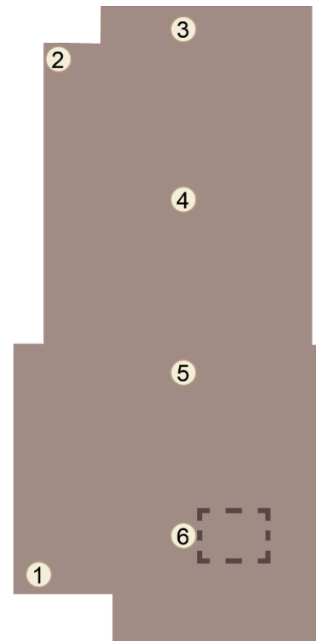

Figure 10. *Thermocouple locations used in the experiments on the front surface. The dashed rectangle shows the area where the TTV is attached on the back surface.*

The simulation model had to be calibrated with a control sample to get better accuracy. The model calibration data was gathered by using a 3 mm thick copper spreader on the experimental setup. This control sample had the same size and shape as the other samples but it was made of solid copper. It was also painted on both sides to get consistent radiative heat transfer conditions for all samples. After the thermocouples were attached as in Figure 10, the heat spreader was placed vertically to the test setup to better correspond to the intended orientation in the application. For this calibration experiment, only 7 W power setting was used.

Many vapor chamber samples were available but only 0.6 mm thick vapor chamber was selected for further characterization. It was noted that this was the most suitable for the application. It had sufficient mechanical stability to withstand handling and assembly of the product. The thinner versions were too fragile as the walls did not provide sufficient support. Furthermore, the thinner vapor chambers had lower performance compared to the 0.6 mm thick one. Also, it was found that the thicker samples provided the same performance as the 0.6 mm thick but they would have required more volume inside the system.

The selected 0,6 mm thick vapor chamber sample was prepared similarly as the control sample. It had its surfaces painted and thermocouples attached with thermal grease and Kapton tape. The vapor chamber was attached to the test setup also vertically to ensure correct gravitational effect and convection around it.

3.2 Simulation setup

To characterize the behavior of the vapor chamber, the experimental results were used as the basis for developing the model. First, the data from the experiments made with the copper spreader was used to calibrate the simulation model with a best-fit method to solve the unknowns in the system. The next step was to run simulations with several conductivity values for multiple power settings in a thin vapor chamber model using the values from the calibration. Comparison of these results with the experimental data gave a normalized error value that varied with conductivity. Conductivities that resulted in the least error were used to form a function that describes the temperature dependent conductivity of the vapor chamber. Lastly, the accuracy of the function was verified by applying it to another vapor chamber experiment and comparing the results to the data.

Commercial CFD code FloTHERM 11 was used to model the test setup. The model was constructed from basic primitives that represented solid materials. Also, no additional air flows or fixed flows were added to the model, as the experiments were also shielded from forced convection. The basic geometry of the model was made to correlate to the experimental setup, and all seven monitor points were at same locations as in the experiments. In addition, one monitor point in the TTV was used. The pressing clamps and the aluminum frame were excluded because their effect to the system was very limited. The simulation model is presented in Figure 11. The picture on the right is an overview of the model, while the picture on the left is a is detailed view around the TTV.

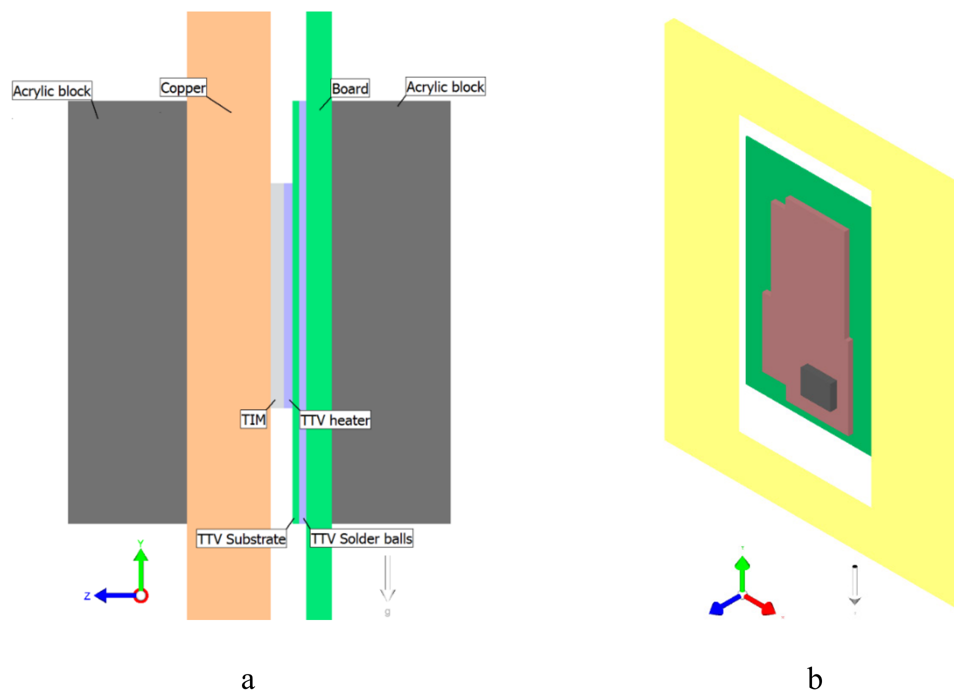

Figure 11. *Simulation setup a) section view from the right at the TTV b) 3D overview of the model*

First the model was calibrated with the 3 mm thick copper sample to solve the unknowns related to the test setup. Copper is a good calibration sample as it has very well-known thermal properties and can therefore be modeled accurately. The calibration simulation was done with a 7 W power setting. The results from the calibration were brought into Excel for processing. A multilinear fitting and solver plug-in were used to calculate the values for the unknowns that resulted in a minimum error to the measurements The unknowns were the emissivity of the paint covering the vapor chamber, PCB conductivity, and thermal interface material conductivity and surface thermal resistivity. A total of 98 different designs, which were created by using design experiments tools, were used in this calculation. The optimized values are shown in the Table 2.

Table 2. *Unknowns solved with the calibration model*

Unknown	***Value***
Emissivity	0.888548
Board conductivity (W/(m K))	40.05669
TIM conductivity (W/(m K))	6
TIM surface impedance ((K m^2)/W)	0.000005

After calibration, the 0.6 mm thick vapor chamber was modeled and the values from the calibration were applied to it. To achieve as accurate results as possible, four layers of grid cells were assigned through the thickness of the vapor chamber. In the xy-direction, the maximum grid cell size was assigned to be 0.8 mm. This was found to be the best for still keeping the model simple but accurate. More layers did not produce more accuracy. The surface of the domain representing the vapor chamber was assigned as a non-metallic paint with emissivity of 0.89.

To find out the best conductivity value for each power setting, a range of thermal conductivity was used. The overall range of values was between 300 W/mK and 11000 W/mK, which was found to cover the whole possible conductivity range. By using the command center interface inside FloTHERM, a simulation case set for each power setting was generated. The conductivity of the material assigned to the vapor chamber was set as a variable, and a linear series of conductivities was given to it. Each conductivity corresponded to one case in the case set. FloTHERM solved the cases and produced a value matrix similar to that obtained from the experiments. Each conductivity value yielded a set of temperatures for the monitor points, which were then compared to the corresponding experimental values.

For the comparison, the root mean square error (RMSE) was used. It is a widely used method to calculate the difference between the model and the experimental data. It tells how much off, on average, the model is from the measurements, and it amplifies the effect of big errors as it weights them more. [45]

4. RESULTS AND CHARACTERIZATION

The experiments produced data, which shows well how differently the vapor chambers react to heat compared to the copper spreaders. In this section, these two different type of spreaders are compared. Also, the data is used to generate the behavioral model to form the simplified and flexible CFD model of the vapor chamber.

4.1 Results from the experiments

The experiments showed that the vapor chamber offers better thermal properties than copper, when heat loads increase over a certain limit. It has lower temperature difference on its surface, and it responded quickly to the changes in the heat input. Figure 12 illustrates the transient behavior of the heat spreaders during a 30 minute period with 7 W heat input. One can see that the vapor chamber reaches its steady state in just 10 minutes, while for copper it takes 30 minutes. This difference is because the mass of the vapor chamber and hence its heat capacity are much smaller than those of copper. [46]

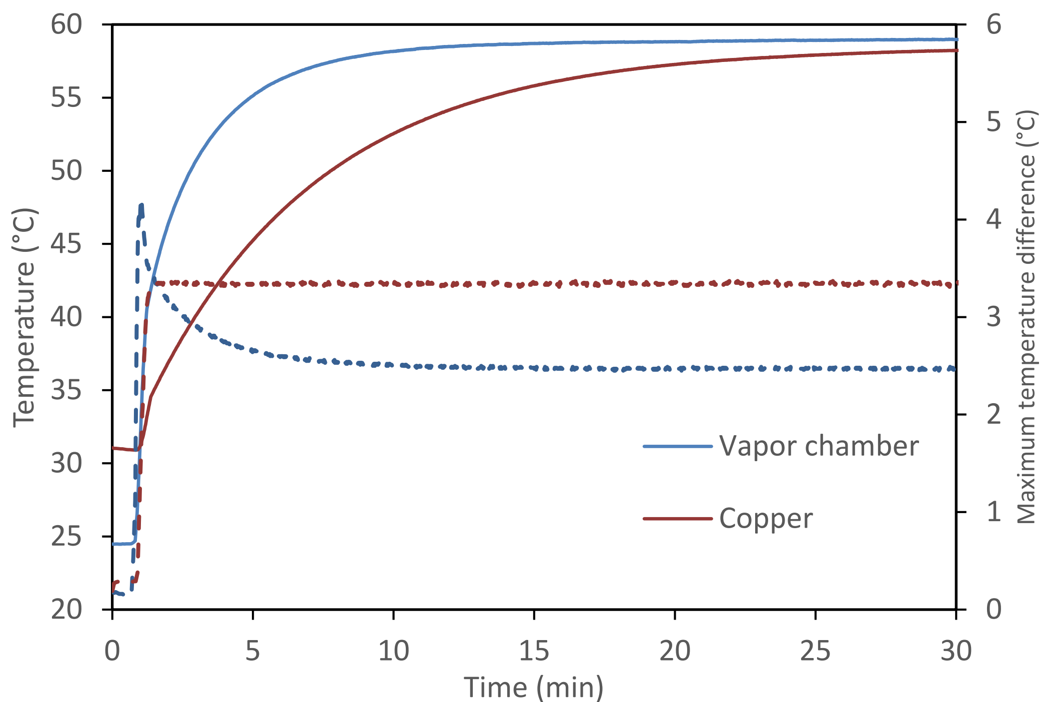

Figure 12. *Thermal response of a vapor chamber and a copper spreader to a heat input change.*

The dashed lines in Figure 12 show the maximum temperature difference on the front surface of a heat spreader, showing that the vapor chamber and the copper spreader are behaving very differently. The copper spreader's temperature gradient is increasing very rapidly as the temperature is increasing. This is consistent with the diffusion theory discussed in section 2.3.

On the other hand, the vapor chamber behavior is opposite: when heat input is activated at t=0, the gradient suddenly increases to its maximum, but when the mass flow inside the vapor chamber increases, the gradient decreases gradually.

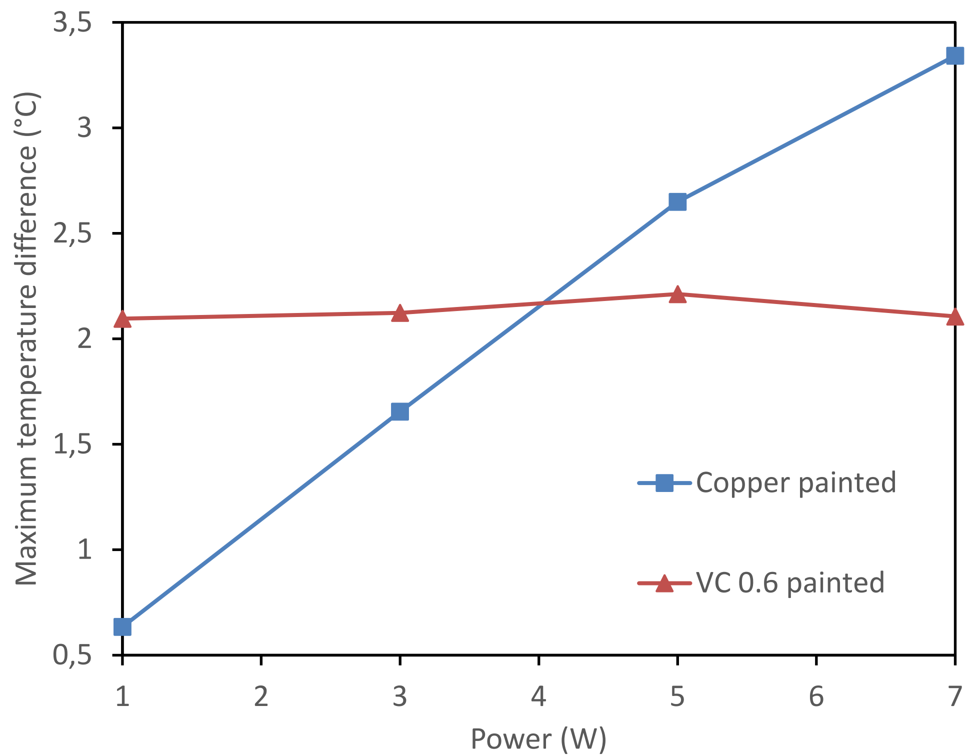

Figure 13. *Maximum temperature difference on the front surface of the heat spreaders*

By using multiple power settings, bigger differences in the temperature gradient can be observed. In Figure 13, the maximum temperature difference is plotted against power. The gradient over the copper spreader clearly increases as a function of power, but for the vapor chamber it stays constant. The average temperature difference over the vapor chamber's surface was 2.3 °C.

The coefficient of thermal spreading (CTS) was also calculated for both spreaders. This number is the ratio of the average surface temperatures and the maximum temperature on the front surface. [44] These values are plotted against power in Figure 14.

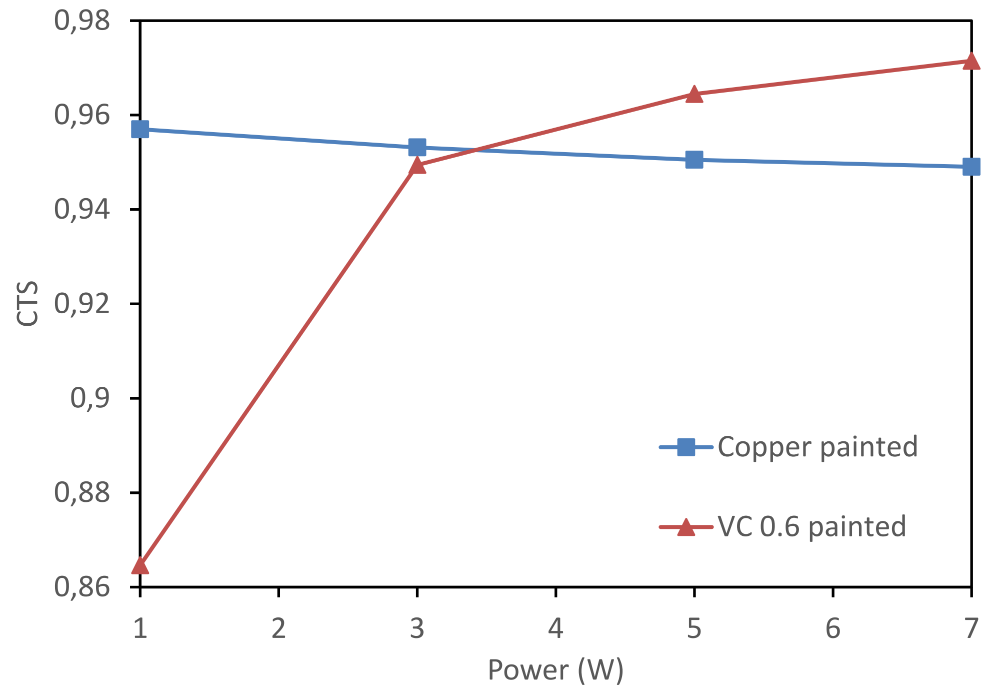

Figure 14. *Coefficient of Thermal Spreading (CTS) for the vapor chamber and for the copper spreader*

The CTS value of copper is showing a fairly constant decrease over the power as the temperature gradient increases. However, the vapor chamber's CTS value starts from a low value and quickly increases over the copper's value as the power increases. This again shows that the vapor chamber's performance is strongly connected to the heat input, as higher power drives vapor further inside the vapor chamber. It should be also noted that the copper spreader shows a good CTS value since here a 3 mm thick solid copper spreader was used. This is a highly unrealistic heat spreader to be used in mobile applications

4.2 Results from the simulation

When the suitable conductivity range was studied, it was noted that after a certain conductivity value no more accuracy could be added to the model. To better investigate this phenomenon, additional simulations were done with an online calculator developed by the Microelectronics Heat Transfer Laboratory at the University of Waterloo. [47] It was used to calculate the spreading resistance for an isotropic conductor of size 135 x 70 x

0.6 mm with a rectangular heat source. The results showed that when conductivity is greater than 5000 W/m K, there is no change in the spreading resistance. This is illustrated in Figure 15, where the spreading resistance is plotted against conductivity.

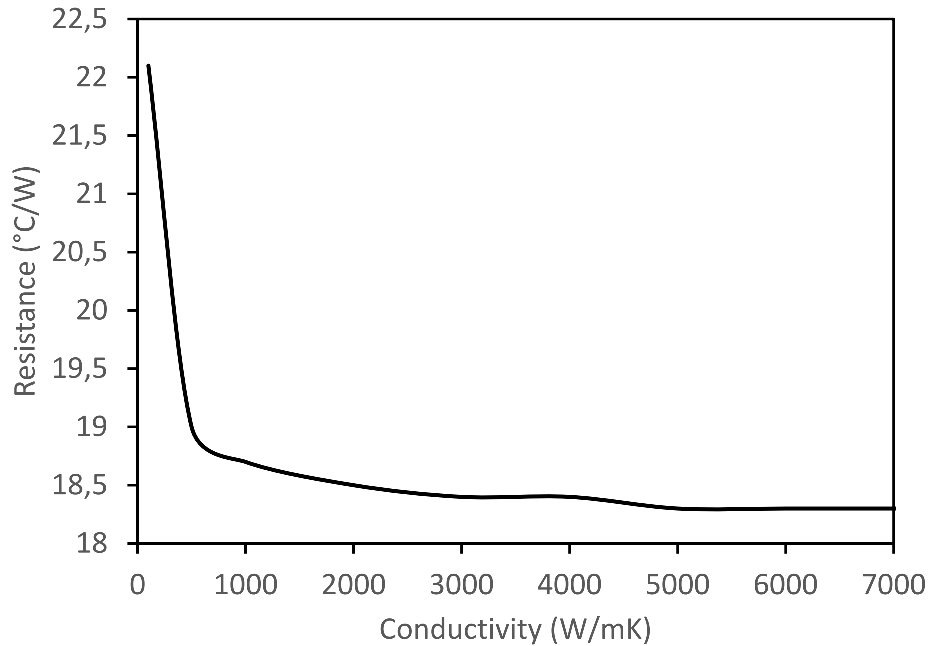

Figure 15. *Spreading resistance against conductivity at 5 W power calculated with MHTL online calculator*

The results from the characterization simulations were exported from FloTHERM to Excel as one table, which was then divided to separate each power setting as its own table. Each table contained a simulation case with a different conductivity value, showing the temperature value at each of the eight monitor points. The corresponding experimental data was added in the table for comparison. From both simulation and experimental data the ambient temperature was subtracted to normalize both data sets to the same level. Then, the delta value for each monitor point was calculated so that the experimental value was subtracted from the simulation value. This was done to each monitor point for each case. Finally, the RMSE value was calculated for each case by using equation 5.

$$RMSE = \sqrt{\frac{\sum_{i=1}^{n}(\Delta T)^2}{n}} \tag{5}$$

Here ΔT is the temperature difference between the simulation and experiment at the monitor point and n is the number of the monitor points. Hence, every conductivity value had a corresponding RMSE value, and the best conductivity value had the smallest error.

The results were normalized to find the best-fit thermal conductivity. This was done by dividing each RMSE value with the minimum value for each power setting. The resulting value for the best-fit conductivity is one, and for other values higher than that. The normalized RMSE values are plotted against conductivity in Figure 16.

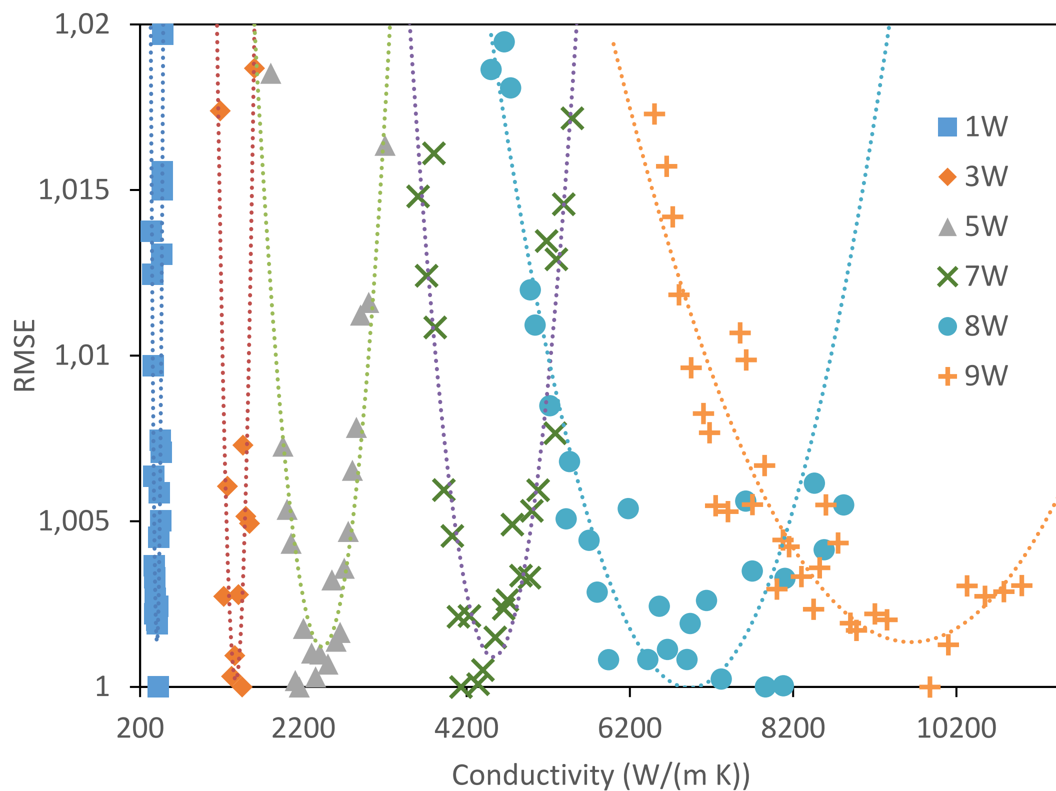

Figure 16. *Normalized RMSE values for each power setting*

One can notice that as the conductivity approaches the optimum, the error value approaches its minimum. Also as the theory predicts, the best-fit conductivity is clearly increasing with power. The erratic behavior seen in Figure 16 may be caused by the fact that the simulations were run as independent cases and they are sensitive to the initial conditions. Similarly, there was some difference between the results from the simulation sets. Furthermore, as described earlier in this section, when conductivity rises the spreading resistance is approaching its smallest possible value. Consequently, bigger change in conductivity is needed to make significant effect to the error. This makes the error curves broader at higher conductivities.

Table 3. Conductivity and heater temperature values calculated from the error functions

Power (W)	k (W/m K)	Heater (°C)
1	406.91	32.01
3	1371.58	42.60
5	2431.02	52.24
7	4525.75	61.10
8	6930.18	65.29
9	9648.61	69.42

To determine more reliably the best conductivity value for each power setting, an error function has to be created. For this, a second-degree polynomial function was fitted to the data in Excel. Because Excel does not support calculations made based on graphical curve fitting, the LINEST-function has to be used. This allows to solve the polynomial coefficients, which can be used to find the minimum values of the functions more accurately. The results are shown in Figure 17.

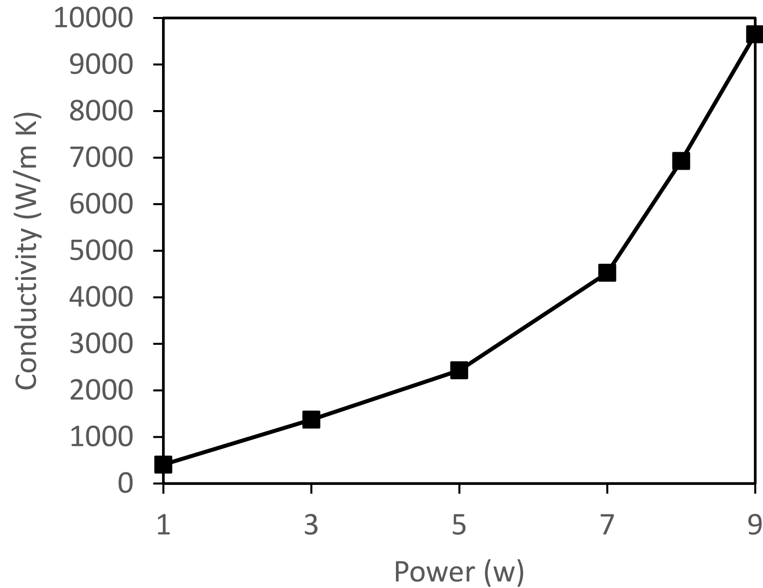

Figure 17. *Best-fit conductivities as a function of power*

The best-fit conductivity values can be plotted against power, as shown in Figure 17. This clearly shows that conductivity follows an exponential increase as power input to the vapor chamber increases. This is also confirmed by studies made by Wei et.al. [1] This

behavior can be explained by the fact that as the power increases, the speed of the vapor also increases and it has to travel farther to find a cooler area, which means that the heat spreading area also increases. This leads to the observed exponential growth.

4.3 Behavioral model of the vapor chamber

To use the information from the previous section in the CFD software, some approximations have to be made. First, the power cannot be used to define the conductivity values, but temperature can be used as a proxy for the power.

After all necessary parameters are characterized, they can be inserted in the CFD software. As many materials have temperature dependent properties, there is a built-in feature in FloTHERM that allows to define these properties. However, it is limited to model only linear temperature dependency. Thus, to use the algorithm, a linear approximation must be made. Since the low power cases are not thermally challenging, and the high power cases will lead to high temperature and therefore high conductivity, an intermediate range of the slope is most useful. The choice of linearization range could be adjusted for other considerations if needed.

In Figure 18, the best-fit conductivities are plotted straight against temperature. The plot is very similar to the power dependence shown in Figure 17. Although the result is exponential, a line can be also fitted to the data. It clearly is not representing well the data that was gathered from the characterization, but this approximation is still suitable for this application. The coefficient of the line will change accordingly if the curve changes its shape.

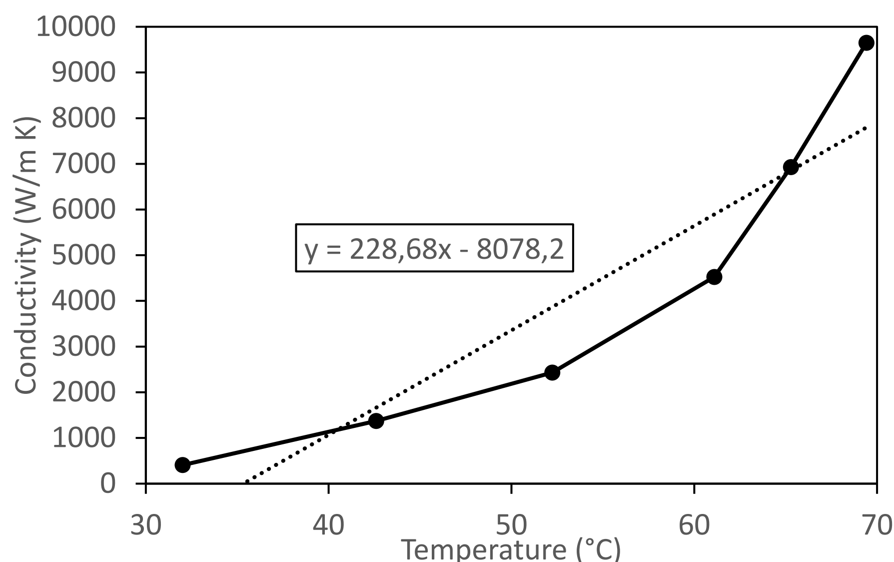

Figure 18. *Conductivity vs. temperature with the linear approximation.*

The meaning of conductivity increase will lose its significance after a certain point. In this case, this point will be somewhere above 60 °C. After this, the conductivity is increasing very rapidly, over 600 W/m K for each 1 °C. For this reason, the steeper part of the curve is less significant, as it is nearly two times the conductivity of copper.

On the other hand, the lower section of the curve shows a smaller increase, depicting the vapor chamber's behavior at lower temperatures. These values are not so interesting since the lower temperatures in hand held devices are not challenging from the thermal design point of view. This means that the presented approximation is sufficient for this application.

4.4 Applying the behavioral model

The behavioral model with parameters determined in the previous section was tested to ensure that it will work. For this purpose, experimental data from a vapor chamber vendor was used as a reference. Similarly to characterization, the experimental setup was replicated into the CFD software. The experimental setup was a different orientation and geometry from the tuning data set. The vapor chamber was modeled with temperature dependent thermal conductivity using values presented in Table 4.

Table 4. *Temperature dependent material model for the vapor chamber*

Property	*Value*
Reference conductivity (W/m K)	6930
Coefficient (W/m K^2)	228.68
Reference temperature (°C)	65.29

The vapor chamber was a 135 x 70 x 0.6 mm rectangle, which means that its geometry was different from the one used in the characterization. This is important since the starting point of this work was to find a more robust modeling method. Also, the surface of the vapor chamber was painted with black paint on its front surface. To measure the surface temperatures, seven thermocouples were attached on both sides of the spreader. Figure 19 shows the locations of the thermocouples.

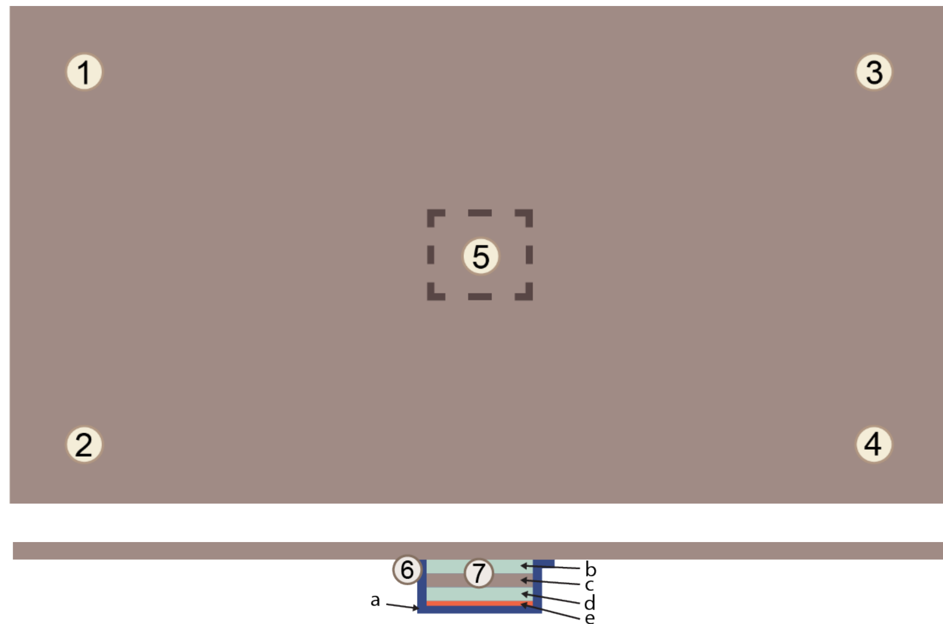

Figure 19. *Thermocouple locations in the validation experiment and simulation. Heater parts: a) vacuum glue and tape b & d) thermal grease c) copper block e) heater element*

The simulations were done with 5 and 10 W power settings in a similar manner as in the experiments. The heater used to generate heat had the dimensions of 10 x 10 mm, and it was placed at the center of the vapor chamber. The heater was thermally connected to the vapor chamber with a copper block and thermal grease. The heater assembly was attached in place with vacuum glue and insulating tape. The sample and the heater were placed horizontally on an insulating layer of fiberglass to insulate the experimental setup from the table. The fiberglass and the table were much bigger than the sample, so they prevented air flow around the sample. This greatly reduced cooling from the back surface of the vapor chamber and the heater area. Ambient temperature during all experiments was between 25.3 and 25.7 °C. The results were normalized to 25 °C to account for the changes in the ambient temperature between the experiments.

The validation model was calibrated also with a copper sample. Similarly, as in the characterization model, this helped to reduce the effects of unknowns in the experiment. In this case these unknowns were conductivities of the thermal grease and the vacuum glue. The experiments were done in free convection so that room ventilation had an effect on the results. This required that a light forced air flow be added to the model to account for air movement over the sample. Design experiments were used to create 20 simulation cases with different flow settings from each side of the simulation space. A combination which produced the smallest RMSE value then was selected.

Two different types of simulations were used in the validation: a control simulation and a simulation model with the behavioral model. To better illustrate the situation where the

thermal designer has not a good understanding of the thermal properties of the vapor chamber, the control simulation had a constant thermal conductivity value. The conductivity value of about 5000 W/m K was considered high enough, as in Section 4.2 it was found that the model will not produce better spreading after 5000 W/m K.

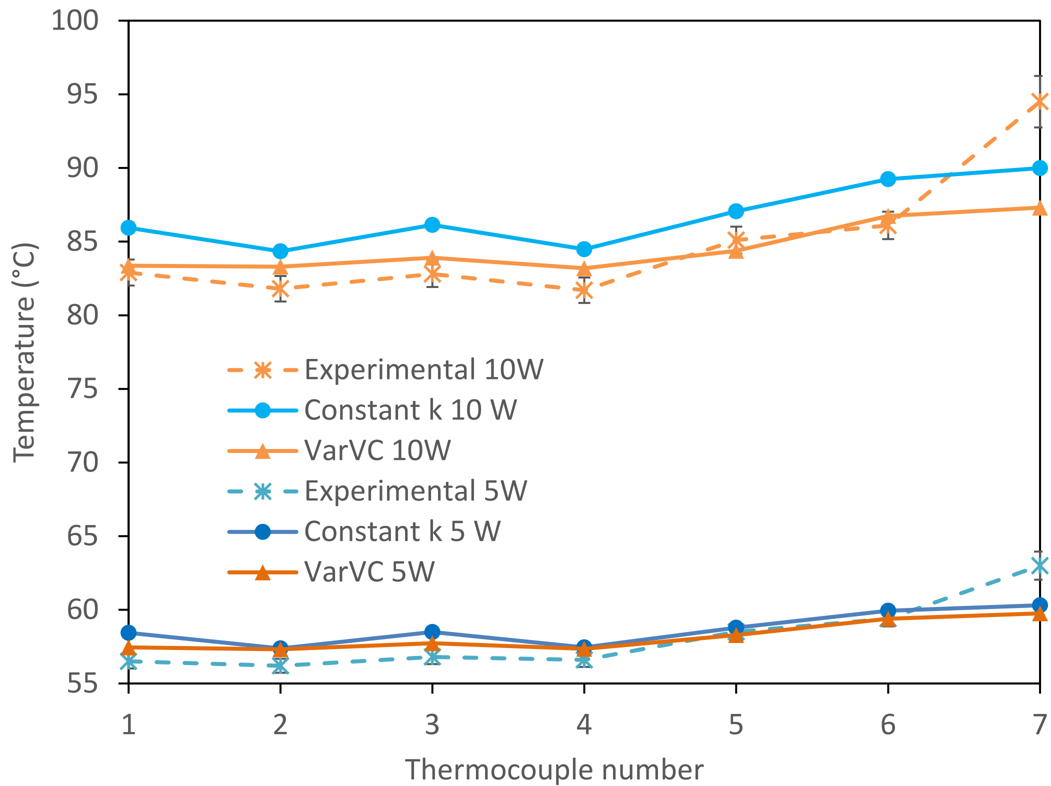

Figure 20. *Results from the validation simulation. Constant conductivity value is 5175 W/m K*

The results from the validation simulation are shown in Figure 20. The results show that both models are in good agreement with the experimental results. However, the constant conductivity model over-predicts temperatures at the outer edges of the vapor chamber with higher power settings. On the other hand, the behavioral model produces consistent result with both power settings. This shows that the behavioral model can be used with different power settings and different vapor chamber geometries. Location 7 is a thermocouple that does not show good agreement. It is most probably because it is so close to the heater that the errors in the heater model are magnified.

With 5 W power setting, both models are producing nearly similar results. This can be explained by calculating the conductivity value for the behavioral model. With average temperature of 58 °C in the vapor chamber model, it produces a conductivity value of 5185.24 W/m K. This is nearly equal to the constant conductivity model. However, when

the power is doubled, the conductivity is also doubled to 11268.13 W/m K. At such high temperatures, the constant conductivity model will not spread heat as effectively as the behavioral model, which has much greater conductivity.

The same simulation was also run with 10000 W/m K constant conductivity. This produced results that showed that both models are giving results very close to each other. This suggests that as the power increases, the constant conductivity model with high conductivity value comes closer to the behavioral model. These values might be different with other vapor chamber geometries as the constant conductivity model is ruled by the fin theory and the behavioral model is not. In other words, much bigger spreader needs more power to drive vapor in the vapor chamber farther, and the constant conductivity model does not take that into account.

Furthermore, with lower power settings the constant conductivity model will model too high conductivities, which results in too good spreading. This will not give accurate results since the temperature gradient is too small and too much heat is going through the spreader. It will lead to incorrect surface temperatures for the system, which gives an overoptimistic picture of the thermal solution. The behavioral model, on the other hand, will adapt to these kind of changes accordingly. As the power decreases and temperatures accordingly, conductivity will also decrease, which will give more realistic results.

Because all measurements were done on a power range where the vapor chamber is producing sufficient vapor motion to spread heat evenly, it has to be noted that the far ends of the operating envelope are not characterized in this work. The startup and the dry out conditions are not modeled correctly by this behavioral model. This is also limited by the modeling technique in the CFD software. Since it is only supporting linear temperature dependencies, sudden changes in the coefficient cannot be included in the model. These changes are mostly a result of the capillary limit of the wick described in section 2.2.3.

In addition, this behavioral model will lose its accuracy if the ambient temperature is changed significantly since the vapor chamber is driven by the temperature difference between the evaporator and the condenser, which is related to the ambient temperature.

5. CONCLUSIONS

Computing power provided by the handheld devices like smartphones and tablets is increasing. Consequently, the heat loads produced by the electronics in the device are also increasing and affecting the external temperature distribution, which users perceive. Vapor chambers are one of the many solutions that can help to make this distribution smoother. They can be made thin so that the overall device thickness is not affected. Since the spreading effect of the vapor chamber is based on phase change and mass flow, they can be complicated to simulate. The focus of this work was to study if a simpler CFD model can be created to make a system level model more efficient to use during product development.

It was shown that significant simplification can be achieved by applying knowledge from the earlier studies. These showed that because the solid components like the wall and the wick are not contributing to the heat transfer as much as the vapor, all components can be modeled by solid conductors. In this type of model, the vapor chamber is constructed of a series of layers, which have thermal conductivity value close to their effective values. However, it was concluded that this method creates very thin layers that can make the model inaccurate. Also, in order to create layers that represent well the particular vapor chamber, one has to have sufficient knowledge about the structure of the vapor chamber. In this case, such information was not available.

The second observation found in the experiments was that the temperature gradient on the surface the vapor chamber is approximately constant over a wide range of heat inputs. In solid materials like copper, the diffusion theory and experiments show that the gradient will increase with increasing heat input.

To simplify the model even more from the layered model, the so-called behavioral vapor chamber model was developed. This model uses one simulation domain or a cuboid to model the geometry and the spreading behavior of the vapor chamber. The goals were to create this model in such a way that it would adapt to the changes in the shape, thickness, and heat input of the vapor chamber. Another goal was, it was a goal to develop a modeling method that can characterize this behavior over likely application parameters.

The experimental data for the characterization was gathered first by using the thermal test vehicle as a heat source. It can produce the wanted heat loads accurately and at the same time the temperature data is logged by the data logger. Six different power settings were used to cover the whole possible range of heat loads. All experiments were done in a still-air chamber that prevented room ventilation from interfering with the air flow around the sample.

Since the CFD model had to be calibrated to obtain the unknowns like paint emissivity, PCB conductivity, TIM conductivity and TIM surface impedance, a copper plate was first used in the experiments. The calibration sample was 3 mm thick and it was made of solid copper. This produced a reliable reference since copper has well known properties and it can be simulated with diffusion. 7 W power setting was used for the calibration measurements.

For the characterization, a 0.6 mm thick copper-water vapor chamber was selected. During the early studies, it was noted that thinner samples were too fragile to handle and they offered too low performance. On the other hand, thicker vapor chambers had the same performance as the selected but they would make the device thicker. Therefore, the 0.6 mm sample was the most suitable for this application.

To get a better idea of the effective conductivity range, an online calculator for the spreading resistance made by Heat Transfer Laboratory at the University of Waterloo was used. This calculator relies on the analytical solutions developed by the laboratory and published in papers. The vapor chamber dimensions were inserted into the calculator, which returned the spreading resistance value for the specific conductivity and power values. It was found that with 7 W power setting the spreading resistance will decrease very rapidly until the effective conductivity of 2000 W/mK is reached. Beyond this value, the resistance will decrease and stabilize at 18.3 °C/W at 5000 W/mK. The result suggests that for each power setting there is a saturation point where maximum spreading is achieved. In other words, the performance of the model is not improved if too high effective conductivity is applied.

The CFD simulation model was based on the experimental setup. First, a model with the reference sample was created to gather calibration data. Good agreement was achieved by trying different values for the unknowns and selecting the combination that produced the smallest error. The selection was done with surface response optimization. The calibrated values were then inserted into the model.

The simulations were continued with the simplified vapor chamber model. A series of simulations was conducted with the same six power settings as the experiments. Also, a range of conductivities was used to find the best-fit value for each power setting. The overall range was from 300 to 11000 /mK. The design experiments tool inside FloTHERM helped to create this set of simulations, and each case was solved independently.

The results from the simulations were compared with the experiments to form an error function for each power setting. First, the normalized RMSE value set was calculated for each power setting. These values were plotted against conductivity and it showed, that the error is following a second degree polynomial function. This information was used to

find the conductivity value that produced the minimum error value in the error set. Results showed that as the power increases, the best-fit conductivity increases.

The second step in the characterization was to plot the conductivities against evaporator temperature. This clearly showed that as the theory predicts, the vapor chamber's effective conductivity increases as a function of the heat source temperature. The rise was found to be exponential, which is supported by literature. [1] Since FloTHERM does not allow to input exponential temperature dependency, a linear approximation had to be made. Although linearization had a big effect on the extreme ends of the temperature range, it was considered to produce a good model since the intermediate range of the slope is the most useful. The low power cases are not thermally challenging and the high power cases will drive the effective conductivity to a high value anyway.

Finally, to validate the model, the resulting temperature dependent thermal conductivity was used to model another unrelated data set to verify its usefulness and accuracy. The used vapor chamber had different geometry and the experiments were conducted on a table without shielding from the room ventilation. Power settings of 5 and 10 W were used. As with the previous data, the model was calibrated with the results from the experiments done with the copper spreader to eliminate the unknowns.

In the CFD software, the calibrated behavioral model, with parameters obtained from the characterization, was used to compare the model to the experiments. In addition, the vapor chamber was modeled with constant conductivity as a comparison to show how well the behavioral model adapts to heat input changes.

The validation confirms that by tuning the behavioral simulation model of a vapor chamber to match the experiments, a simpler model can be achieved. The model will be more flexible than the models with constant conductivity, as it will react to temperature changes as a real vapor chamber might do. The validation also shows that the behavioral model can be used to simulate different sized vapor chambers with the same parameters.

Overall results of this work show that even without detailed knowledge about the vapor chamber that is modeled, a very simple behavioral model can be created. The root-mean-squared error minimization a creates function that describes how the vapor chamber reacts to power and temperature changes. Simulating a vapor chamber simply by using a thermal conductivity as a function of temperature is a useful way to include the spreading behavior of the vapor chamber in a complex system model.

The behavioral model is more flexible than the constant conductivity model with high thermal conductivity, as it can adapt to wider temperature changes. For product development, it is very useful that this model allows the vapor chamber geometry to be changed. The biggest limitations of the behavioral model are that the model is not suitable to simulate the startup and dry out conditions since at these stages the vapor chamber behavior is not linear. Also, changes in the ambient temperature will affect the accuracy of the

model. In addition, it is expected that the transient behavior is not modeled correctly as overall density and effective heat capacity were not investigated.

The behavioral model offers a good solution for the vapor chamber simulation, when a mathematical compact model cannot be used or is not wanted. This can be the case with commercial CFD software that could require modifications or add-ons to incorporate a new model. In addition, since the behavioral model is based only on changing thermal conduction, it is easy for an engineer who is using it to understand and change all parameters. Furthermore, because there is a small number of parameters involved in the system, the thermal designer and a vapor chamber supplier may communicate better about the characteristics of a vapor chamber. Often the manufacturers don not want to share the details about their design, which makes work of a thermal designer difficult since the vapor chamber's behavior is hard to guess. The results of this work enable the manufacturers to give out the vapor chamber's properties without revealing their intellectual property. The thermal designer can then use them in the simulations during the product design cycle.

REFERENCES

[1] X. Wei, K. Sikka, Modeling of vapor chamber as heat spreading devices, Thermal and Thermomechanical Proceedings 10th Intersociety Conference on Phenomena in Electronics Systems, 2006. ITHERM 2006. IEEE, pp. 578-585.

[2] Y. Chen, K. Chien, T. Hung, C. Wang, Y. Ferng, B. Pei, Numerical simulation of a heat sink embedded with a vapor chamber and calculation of effective thermal conductivity of a vapor chamber, Applied Thermal Engineering, Vol. 29, No. 13, 2009, pp. 2655-2664.

[3] M.P. Rumpfkeil, Computational Fluid Dynamics (CFD), University of Dayton, web page. Available (accessed 8.6.2016): http://academic.udayton.edu/markusrumpfkeil/cfdcourse/intropresentation.pdf

[4] R. Bhaskaran, L. Collins, Introduction to CFD basics, Cornell University-Sibley School of Mechanical and Aerospace Engineering, 2002.

[5] A. Luikov, Conjugate convective heat transfer problems, International Journal of Heat and Mass Transfer, Vol. 17, No. 2, 1974, pp. 257-265.

[6] Commercial codes, CFD Onlina, web page. Available (accessed 20.6.2016): http://www.cfd-online.com/Wiki/Codes#Commercial_codes.

[7] FloTHERM Background Theory Reference Guide, Mentor Graphics, web page. (accessed 1.11.2015).

[8] R.S. Gauger, Heat transfer device, US 2350348 A, (6.6.1944).

[9] G.M. Grover, Evaporation-condensation heat transfer device, US 3229759 A, (18.1.1966).

[10] B. Suman, Modeling, experiment, and fabrication of micro-grooved heat pipes: an update, Applied Mechanics Reviews, Vol. 60, No. 3, 2007, pp. 107-119.

[11] Vapor Chambers, MyHeatSinks Pte. Ltd, web page. Available (accessed 18.8.2016): http://www.myheatsinks.com/heat-pipe-solutions/vapor-chambers/.

[12] P.D. Dunn, D. Reay, Heat pipes, 6th ed. Elsevier, 2014.

[13] B. Xiao, A. Faghri, A three-dimensional thermal-fluid analysis of flat heat pipes, International Journal of Heat and Mass Transfer, Vol. 51, No. 11, 2008, pp. 3113-3126.

[14] R. Ranjan, J.Y. Murthy, S.V. Garimella, U. Vadakkan, A numerical model for transport in flat heat pipes considering wick microstructure effects, International Journal of Heat and Mass Transfer, Vol. 54, No. 1, 2011, pp. 153-168.

[15] Vapor Chamber Assemmlies, Advanced Cooling Technologies, Inc., web page. Available (accessed 6.10.2016): https://www.1-act.com/products/vapor-chamber-assemblies/.

[16] D. Reay, P.D. Dunn, Heat Pipes, 3rd ed. 1982.

[17] F. Korn, Heat pipes and its applications, Heat and Mass Transport, Project Report, 2008.

[18] C. Li, G. Peterson, Y. Wang, Evaporation/boiling in thin capillary wicks (l) - Wick thickness effects, Journal of Heat Transfer, Vol. 128, No. 12, 2006, pp. 1312-1319.

[19] R.S. Prasher, A simplified conduction based modeling scheme for design sensitivity study of thermal solution utilizing heat pipe and vapor chamber technology, Journal of Electronic Packaging, Vol. 125, No. 3, 2003, pp. 378-385.

[20] A. Faghri, S. Thomas, Performance characteristics of a concentric annular heat pipe: Part I - Experimental prediction and analysis of the capillary limit, Journal of heat transfer, Vol. 111, No. 4, 1989, pp. 844-850.

[21] A. Faghri, Heat Transfer Limitations of Heat Pipes, Global Digital Central, web page. Available (accessed 20.8.2016): https://www.thermalfluidscentral.org/encyclopedia/index.php/Heat_Transfer_Limitations_of_Heat_Pipes.

[22] E. Levy, Theoretical investigation of heat pipes operating at low vapor pressures, Journal of Engineering for Industry, Vol. 90, No. 4, 1968, pp. 547-552.

[23] C. Tien, K. Chung, Entrainment limits in heat pipes, AIAA Journal, Vol. 17, No. 6, 1979, pp. 643-646.

[24] D. Scott, P. Garner, Heat Pipes for Electronics Cooling Applications, 3, Vol. 2, No. Electronics Cooling magazine, Sep 1st, 1996, pp. 14.7.2016.

[25] A.A. Attia, B.T. El-Assal, Experimental investigation of vapor chamber with different working fluids at different charge ratios, Ain Shams Engineering Journal, Vol. 3, No. 3, 2012, pp. 289-297.

[26] A. Basiulis, R. Prager, T. Lamp, Compatibility and reliability of heat pipe materials, AIAA 10th Thermophysics Conference, Denver, CO.

[27] Compatible Fluids and Materials, Advanced Cooling Technologies, Inc., web page. Available (accessed 29.8.2016): https://www.1-act.com/compatible-fluids-and-materials/.

[28] P. De Gennes, F. Brochard-Wyart, D. Quéré, Capillarity and wetting phenomena: drops, bubbles, pearls, waves, Springer Science & Business Media, 2013.

[29] S. Wong, Y. Lin, Effect of copper surface wettability on the evaporation performance: Tests in a flat-plate heat pipe with visualization, International Journal of Heat and Mass Transfer, Vol. 54, No. 17, 2011, pp. 3921-3926.

[30] P. Perrot, A to Z of Thermodynamics, Oxford University Press on Demand, 1998.

[31] J. Corman, Engineering Design of Heat Pipes, 1971.

[32] T.M. Tritt, Thermal conductivity: theory, properties, and applications, Springer Science & Business Media, 2005.

[33] A. Faghri, Working Fluids and Temperature Ranges of Heat Pipes, Global Digital Central, web page. Available (accessed 1.9.2016): http://www.thermalfluidscentral.org/encyclopedia/index.php/Working_Fluids_and_Temperature_Ranges_of_Heat_Pipes#cite_ref-FR2012_0-0.

[34] W. Qu, Progress Works of High and Super High Temperature Heat Pipes, INTECH Open Access Publisher, 2011.

[35] H. Kreeb, M. Groll, P. Zimmermann, Life test investigations with low temperature heat pipes, Oct 1973, First International Heat Pipe Conference, Stuttgart.

[36] Melting temperatures of some common metals and alloys, The Engineering ToolBox, web page. Available (accessed 30.9.2016): http://www.engineeringtoolbox.com/melting-temperature-metals-d_860.html

[37] D. Reay, R. McGlen, P. Kew, Heat pipes: theory, design and applications, Butterworth-Heinemann, 2013.

[38] MONEL alloy 400, Special Metals Corporation, 2005.

[39] Ammonia-Charged Aluminum Heat Pipes with Extruded Wicks, Nasa, web page. Available (accessed 6.9.2016): http://llis.nasa.gov/lesson/698.

[40] E. Baker, Prediction of long-term heat-pipe performance from accelerated life tests. AIAA Journal, Vol. 11, No. 9, 1973, pp. 1345-1347.

[41] M. Connors, Vapor chambers in blade server CPU cooling solutions, ASME 2007 InterPACK Conference collocated with the ASME/JSME 2007 Thermal Engineering Heat Transfer Summer Conference, American Society of Mechanical Engineers, pp. 703-705.

[42] Ultra Thin Vapor Chamber Test, Asia Vital Components Co. LTD., 2015.

[43] R. Wang, J. Wang, T. Chang, Experimental analysis for thermal performance of a vapor chamber applied to high-performance servers, Journal of Marine Science and Technology, Vol. 19, No. 4, 2011, pp. 353-360.

[44] V. Chiriac, S. Molloy, J. Anderson, K. Goodson, A Figure of Merit for Smart Phone Thermal Management, Electronics COOLING, 2015.

[45] T. Chai, R.R. Draxler, Root mean square error (RMSE) or mean absolute error (MAE)? - Arguments against avoiding RMSE in the literature, Geoscientific Model Development, Vol. 7, No. 3, 2014, pp. 1247-1250.

[46] C. Biber, M. Carbone, Correspondence, 31.3.2016.

[47] Microelectronics Heat Transfer Laboratory, Department of Mechanical Engineering, University of Waterloo, web page. Available (accessed 25.4.2016): http://www.mhtlab.uwaterloo.ca/intro_rect.html.